Depth of focus of the human eye - The transfer from objective data to subjective perception

Dissertation

der Mathematisch-Naturwissenschaftlichen Fakultät
der Eberhard Karls Universität Tübingen
zur Erlangung des Grades eines
Doktors der Naturwissenschaften
(Dr. rer. nat.)

vorgelegt von
Alexander Leube
aus Schleiz

Tübingen
2018

Gedruckt mit Genehmigung der Mathematisch-Naturwissenschaftlichen Fakultät der Eberhard Karls Universität Tübingen.

Tag der mündlichen Qualifikation: 28.06.2018

Dekan:	Prof. Dr. Wolfgang Rosenstiel
1. Berichterstatter:	Prof. Dr. Frank Schaeffel
2. Berichterstatter:	Prof. Dr. Siegfried Wahl

Contents

1 Introduction **7**

1.1 Motivation 7

1.2 The optics of the eye 9

1.2.1 Fourier description of optical aberrations 10

1.2.2 Aberrometry to assess the wavefront errors of the eye 12

1.2.3 Wavelength dependence of aberrations 15

1.3 The human visual system - From the image to perception 16

1.3.1 Hierarchical organization of visual perception 16

1.3.2 Assessment of visual perception 17

1.4 Image quality metrics in vision science 19

1.5 Perceptual depth of focus 21

2 Objectives **22**

3 Subjective depth of focus and induced astigmatic aberration **23**

3.1 Abstract 23

3.2 Introduction 23

3.3 Methods 25

3.3.1 Study protocol 25

3.3.2 Subjective measurements 26

3.3.3 Threshold definition and analysis of defocus curves 27

3.4 Results 29

3.4.1 Residual accommodation and pupil diameter 29

3.4.2 Depth of focus with induced astigmatism 29

3.5 Discussion 31

3.5.1 Depth of focus with induced astigmatism 31

3.5.2 Limitations of the study 34

3.6 Conclusion 34

4 Neural transfer function and its influence on the prediction of subjective depth of focus **35**

4.1 Abstract 35

4.2 Introduction 35

4.3 Methods 37

4.3.1 Participants 37

4.3.2 Protocol 37

4.4 Results . . . 41
4.4.1 Calculation of objective depth of focus from standard parameter 41
4.4.2 Parameter A - The influence of residual lower order aberrations 41
4.4.3 Parameter B The influence of the individual neural transfer function (iNTF) . . . 42
4.5 Discussion . . . 44
4.5.1 Objective depth of focus and image quality metrics . . . 44
4.5.2 Pupil size dependency . . . 45
4.5.3 Monochromatic and polychromatic aberrations . . . 46
4.5.4 Individual neural transfer function iNTF . . . 47

5 Sign-dependent response to spherical defocus under monochromatic light conditions 49
5.1 Abstract . . . 49
5.2 Introduction . . . 49
5.3 Methods . . . 51
5.3.1 Participants . . . 51
5.3.2 Protocol . . . 51
5.3.3 Analysis . . . 53
5.4 Results . . . 53
5.4.1 Chromatic change of refraction and residual accommodation . . 53
5.4.2 Reduction of visual acuity with spherical defocus . . . 53
5.4.3 Comparison between real and simulated blur (observer vs. source method) . . . 54
5.5 Discussion . . . 55
5.5.1 Depth of focus, luminance and higher order aberrations . . . 56
5.5.2 Implications for the emmetropization of the eye . . . 58
5.6 Conclusion . . . 59

6 Summary 60

7 Zusammenfassung 62

8 References 64

9 Publications, conference contributions and talks related to this work 80
9.1 Peer reviewed publications 80
9.2 Peer reviewed conference contributions 81
9.3 Peer reviewed talks 82
9.4 Non peer reviewed talks 82

10 Statement of own contribution 83
10.1 Publication 1 - The influence of induced astigmatism on the depth of focus 83
10.2 Publication 2 - Individual neural transfer function affects the prediction of subjective depth of focus 83
10.3 Publication 3 - Symmetric visual response to positive and negative induced spherical defocus under monochromatic light conditions 84

11 Acknowledgements 85

Acronyms list

AFC	alternative forced choice
ATR	against the rule astigmatism
ANOVA	analysis of variance
BestPEST	best parameter estimation for sequential testing
CCD	charge-coupled device
CSF	contrast sensitivity function
cpd	cycles per degree
DoF	depth of focus
FrACT	Freiburg acuity and contrast test
FHWM	full width at half maximum
GRIN	gradient refractive index
HOA	higher order aberrations
iNTF	individual neural transfer function
IOL	intra ocular lens
IQM	image quality metrics
LCA	longditudal chromatic aberration
LGN	lateral geniculate nucleus
LOA	lower order aberrations
logMAR	logarithm of the minimum angle of resolution
MTF	modulation transfer function
NTF	neural transfer function
PTF	phase transfer function
PSF	point spread function
PAL	progressive addition lens
oDoF	objective depth of focus
OLED	organic light emitting diode
OTF	optical transfer function
rLoA	residual lower order aberrations
SE	mean spherical equivalent refractive error

SEM	standard error of the mean
SF	spatial frequency
sDoF	subjective depth of focus
SQRI	square root integral
TCA	transverse chromatic aberration
VA	visual acuity
VSMTF	visual Strehl of the modulation transfer function
VSPSF	visual Strehl of the point spread function
VSOTF	visual Strehl of the optical transfer function
WTR	with the rule astigmatism

1 Introduction

1.1 Motivation

Systematic analysis of epidemiological data revealed that uncorrected distance refractive error is the most prevalent cause of visual impairment worldwide [Bourne et al., 2013; Resnikoff et al., 2008; Naidoo et al., 2016] and according to the World Health Organization a number of around 153 million people do not have access to a basic optometry services [WHO, 2006]. An even more prevalent visual impairment is caused by uncorrected near vision due to presbyopia with a estimated number of people who have no access to near spectacles with over 500 millions, mainly from less- or least developed countries in the world [Holden et al., 2007, 2008]. Presbyopia refers to the loss of near focusing ability, called accommodation, due to the age-related decrease of the elasticity of the crystalline lens and the capsule [Bennett and Rabbetts, 1998]. This loss of clear near vision leads to a reduction of the quality of life [Goertz et al., 2014; Lu et al., 2011]. However, the depth of focus of the eye is increasing with age [Mordi and Ciuffreda, 1998] due to a smaller pupil size [Winn et al., 1994] and an increase of ocular aberrations [McLellan et al., 2001] and can provide a natural visual support for uncorrected near vision. The thesis is motivated by the high number of persons affected by the loss of clear near vision and the resulting reduction of the quality of life, since near task as reading or handwork are essential for the well-being of individuals.

In the clinical assessment and for the correction of presbyopia, the depth of focus plays a major role. It describes the perceptual tolerance of the visual systems to retinal blur and therefore determines the subjective judgment of refractive errors for instance during a subjective refraction [Tucker and Charman, 1975] or the precision of accommodation [Wang and Ciuffreda, 2006]. Furthermore, the depth of focus affects the goodness of optical corrections for presbyopia since it limits the tolerable amount of unwanted aberrations or the effectiveness of multifocal corrections like intra ocular lenses or contact lenses [Wang and Ciuffreda, 2006].

Until now, the subjective depth of focus cannot be predicted from objective measures [Benard et al., 2011; Legras et al., 2012]. Individual predictions on the tolerance to blur could lead to improved objective techniques regarding the assessment and design of corrective solutions for presbyopia and could therefore enhance the satisfaction level during daily near task for an aging society. Individual predictions have to include optical and neuronal factors [Campbell and Green, 1965] of visual perception. Besides the application of prediction algorithms, for instance, for the calculation of individually optimized refractive power of intraocular lenses or individualized optical designs of progressive addition lenses, predictions of the subjective depth of focus could be used in objective instruments to measure the refractive errors of the eye. Previous approaches to improve presbyopia corrections have resulted in a reduction of the required addition power for near vision, but reduced visual acuity and contrast sensitivity over the entire spatial frequency range and at all viewing distances. New possibilities for the correction of presbyopia have to be applied to different types of corrections, e.g., glasses, contact lenses, intraocular lenses or refractive surgery, without an reduction of visual performance of the eye like visual acuity, stereoscopic sharpness, contrast sensitivity. Using an induced aberration, like defocus, astigmatism or higher order aberration, that balances the increase of the depth of focus and a reduction of visual acuity could reduce addition power of presbyopia corrections like progressive addition lenses. However, an individualized balance between a reduction of visual performance due to unwanted optical aberrations and the requirement of a comfortable near vision depend on the individual tolerance to blur. Novel treatment approaches could further incorporate individualized prediction algorithms to improve individual prognosis on the habituation to optical treatments.

1.2 The optics of the eye

The main refractive components of the human eye are the cornea and the crystalline lens (Figure 1). The cornea, consisting of collagen fibrils, which are structured in the optically transparent layer, the *stroma*, provide next to 75 % [Atchison and Smith, 2000] of the optical power of the accommodation relaxed eye, and is a mechanical integrity [Guarnieri, 2014] that protects the eye's inner structures from physical and chemical influences. In a first approximation the optics of the cornea can be described as a spherical surface with an anterior mean radius of curvature of $R = 7.80\,\text{mm}$ and a mean optical power of $F = 48.0\,\text{D}$. However, in a more detailed analysis, the cornea has to be calculated as an asphere since the radius of curvature increases with the distance from the surface apex [Atchison and Smith, 2000]. The second structure providing a major contribution to the refraction of light in the eye is the crystalline lens. Due to the appositional growth from the lens epithelium where the cells are produced and laid down over existing fiber cells [Augusteyn, 2007] throughout life span, the crystalline lens is structured in layers and consisting of a gradient refractive index, depending on the distance from the lens equator [Glasser et al., 2001; Charman et al., 2012] which is important for the understanding of the optical behavior of the eye. The ability of the eye to vary its focus, namely accommodation, on different object distances depend strongly on the elasticity of the crystalline lens [Charman, 2008]. The tension of the ciliary muscle causes the zonular fibers to relax the lens' shape towards a more round shape with an increase in optical power [Helmholtz, 1867]. Due to the loss of elasticity with aging of the crystalline lens, the ability to focus near objects is reduced and is referred to presbyopia.

Additionally to the two main refractive components, the optics of the eye are further described by the aperture stop that is formed by the iris and called pupil. In a physical description, the aperture stop together with the focal length of an optical system determine the cone angle of incoming light rays [Pedrotti et al., 2007] and therefore, in case of the human eye, the size of pupil determines the retinal illumination. Additionally, the pupil size restrict the impact of optical errors. When the focus of the eye is shifted towards closer targets, the pupil starts to constrict and both eyes converge to cross in the near target distance. This near pupil reflex was shown to increase with age [Kadlecova et al., 1958; Schaeffel et al., 1993] since ability of accommodation decreases and the smaller pupil size could increase the depth of focus [Campbell, 1957].

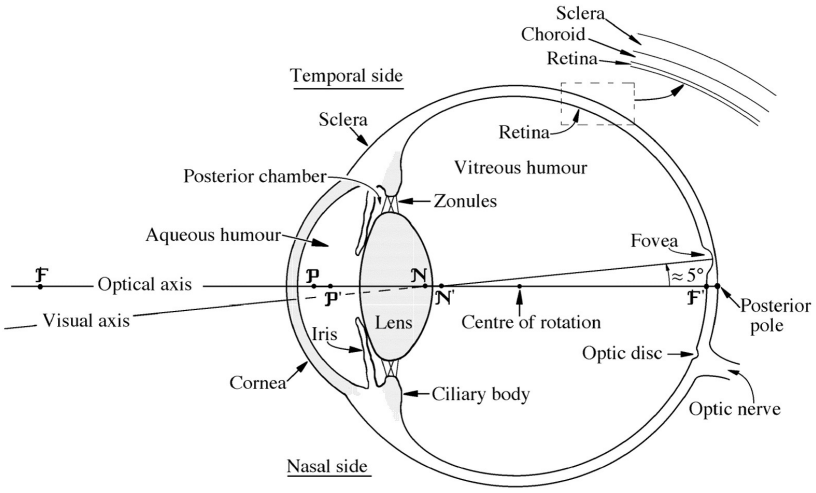

Figure 1: Schematic horizontal section of the optical structures of the human eye. From Atchison [Atchison and Smith, 2000].

Alvar Gullstrand, a Swedish ophthalmologist, first described the normal dimensions of the human eye [Gullstrand, 1924] which has an axial length, measured from the corneal apex to the retina, see Figure 1, of $l = 24.38\,\text{mm}$ and an according total power of $F = 58.63\,\text{D}$. The refractive state of the eye, described as the match between axial length and total refractive power, determines the major refractive error of the eye: spherical ametropia. In case that the refractive power is too high or the eye ball is to long, the light rays are focused in front of the retina and the eye is myopic. If the eye ball is to short or the total power is too low, the eye is hyperopic and the light rays are focused behind the retina plane. [Atchison and Smith, 2000] Myopia and hyperopia result in a rotational symmetric, blurred retinal image. If the refractive power varies with the azimuthal meridian, the refractive error is referred to as astigmatism. These three kinds of refractive errors can be corrected by using optical solutions, such as PAL, contact lenses or IOL.

1.2.1 Fourier description of optical aberrations

The description of light as a ray with a given wavelength and direction traveling from the source of light in space is an assumption and holds true if the wavelength is small compared to the optical components [Pedrotti et al., 2007]. This assumption could be used to explain several phenomena of optics like refraction or reflexion. For the description of e.g. diffraction, the wavelength cannot be neglected and the general case of geometrical optics is described by the wave form of light, first developed 1690 by Christiaan Huygens in "Tractatus de lumine" [Huygens, 1690]. A more general definition of light as a part of the electromagnetic spectrum was later developed by James Clark Maxwell and led to the todays accepted theory of the wave-particle dualism.

As an electromagnetic wave, propagation of light can be described by as a sinusoidal function and therefore the image $I(X,Y)$ from an extended object $O(x,y)$ in space can be calculated using the Fourier approach from signal theory [Pedrotti et al., 2007; Goodman and Gustafson, 1996]. An optical system acts as an Fourier-transformer, where the diffraction pattern of the object is represented by the two-dimensional Fourier transform or the frequency spectrum f_x, f_y of this object. For incoherent light sources, the frequency analysis assumes a linear mapping of different intensities in the (x,y)-space. In the case of an aberration-free optical system the (amplitude) point spread function $PSF(x,y)$ (Equation 1) consists of the Fraunhofer diffraction pattern of the exit pupil [Goodman and Gustafson, 1996]. This allows a direct incorporation of aberrations as wavefront errors $W(x,y)$ as an optical path difference (see Figure 2a) into the pupil function $P(x,y)$ using the wave number $k = 2\pi/\lambda$ (Equation 2).

$$PSF(x,y) = |\mathcal{F}(P(x,y))|^2 \tag{1}$$

$$P(x,y) = A(x,y)\, exp(j\, k\, W(x,y)) \tag{2}$$

$$OTF(f_x,f_y) = \mathcal{F}(PSF(x,y)) \tag{3}$$

$$MTF(f_x,f_y) = |OTF(f_x,f_y)| \tag{4}$$

$$PTF(f_x,f_y) = \tan^{-1}\left(\frac{\Im(OTF(f_x,f_y))}{\Re(OTF(f_x,f_y))}\right) \tag{5}$$

As the point spread function $PSF(x,y)$ describes the intensity distribution in the image plane, the Fourier transform of this function is the optical transfer function $OTF(f_x,f_y)$ (Equation 3). The modulus of the complex valued $OTF(f_x,f_y)$ is defined as modulation transfer function $MTF(f_x,f_y)$ (Equation 4) and the argument as the phase transfer function $PTF(f_x,f_y)$ (Equation 5). The optical transfer function, since it represents a normalized autocorrelation function, equals 1.0 for the zero-frequency condition and is always lower 1.0 for higher spatial frequencies [Goodman and Gustafson, 1996]. These properties show that the OTF describes only relative information of contrast transfer of an optical system and no information on absolute intensity levels. Information on contrast transfer through an optical system, characterized by the $OTF(f_x,f_y)$, can further be used for numerical simulations of images. Since the

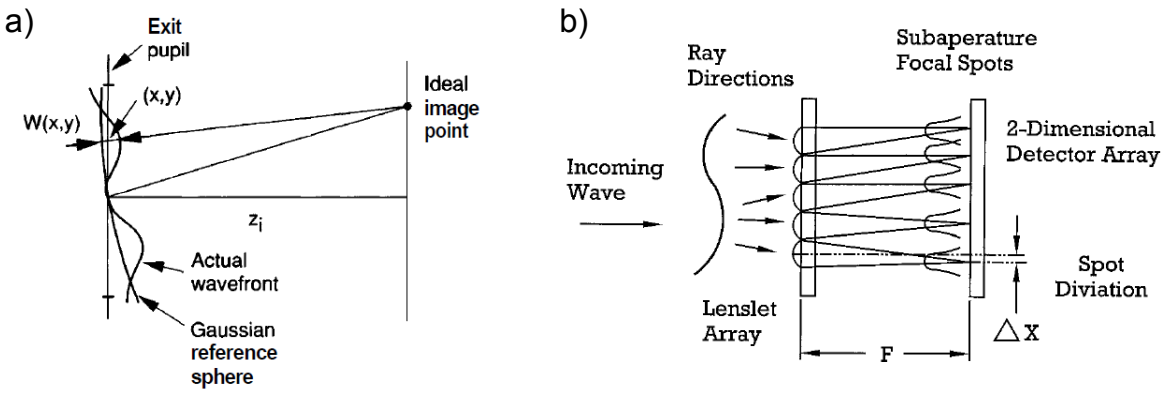

Figure 2: a) Wavefront error $W(x, y)$ defined as the optical path difference between Gaussian reference sphere and the actual wavefront measured in the exit pupil; from [Goodman and Gustafson, 1996]. b) Schematic drawing of the Shack-Hartmann principle to divide the actual wavefront in sub-apertures by a lenslet array. The spot deviation Δx is proportional to the slope of the wavefront. From Platt et al. [Platt and Shack, 2001].

$PSF(x, y)$ describes the transformation of a point from the object space to the image space, the convolution of a spatially extended object with the $PSF(x, y)$ results in the spatial intensity distribution of the image $I(x, y) = O(x, y) \circledast PSF(x, y)$ [Pedrotti et al., 2007].

1.2.2 Aberrometry to assess the wavefront errors of the eye

Describing optical errors as an error between an ideal and an actual wavefront requires to measure the local slope of the wavefront. A technical solution to assess the slope of a wavefront of the human eye [Liang et al., 1994] that was originally developed to improve astronomical observation [Shack and Platt, 1971; Hartmann, 1900] is the Shack-Hartmann sensor. Figure 2b shows a schematic drawing of a Shack-Hartmann wavefront sensor that consist of a lens array with micro lenses and a CCD-chip as sensor. The micro lenses divide the global wavefront from the exit pupil into sup-apertures and focus them on the sensor. For an ideal plane wavefront, all focal points of the sub-apertures are centered in x, y direction. If the slope of the actual wavefront was different from zero, the focal spot deviation would be different from zero as well. This spot deviation is directly proportional to the slope of the wavefront and the global wavefront can be reconstructed with an accuracy that depends on the diameter and number of micro lenses.

Another technical solution to determine the optical transfer properties of the eye was described by Santamaria and colleagues (1987) where they used aerial images from the reflection of a point source on the retina [Santamaría et al., 1987]. Furthermore, laser ray tracing [Navarro and Losada, 1997] where unexpanded laser beams are spotted through different pupil locations and evaluated regarding their lateral displacement could be used to objectively record the aberrations in the living human eye.

Standard analytical description of wavefront errors in ophthalmology and optometry [Thibos et al., 2002b] is performed using a sequence of polynomials that are orthogonal on the unit disk and were first described by Frits Zernike. Normalized pupil coordinates x and y are transformed into the polar coordinates ρ and θ and the polynomials $Z_n^m(\rho, \theta)$ are defined as the product of a radial function $R_n^{|m|}$ and a normalization factor N_n^m, both characterized by the radial order n and the azimuthal frequency m. The eye's wavefront errors are reconstructed by weighting the base function $Z_n^m(\rho, \theta)$ with a coefficient c_n^m. The advantages of using Zernike polynomials are their orthogonality and the fact that they include some of the classical Seidel aberrations, like the second order terms for defocus (Z_0^2) and astigmatism (Z_2^{-2}, Z_2^2). Figure 3 shows the first 36 Zernike polynomials for a radial order from n = 0 to n = 7 and azimuthal frequencies from m = -7 to m = 7. Since Zernike polynomials are independent from each other, the coefficients c_n^m can be evaluated and compared throughout individuals. However, these coefficients are scale, translation and rotation invariant. Therefore, in statistical analysis of ocular aberrations it is important that wavefront errors are compared for the same pupil size, the same wavelength and the same pupil location [Thibos et al., 2002b; Bara et al., 2006]. To transform the measured Zernike coefficients to a common frame, different methods can be applied [Schwiegerling, 2002; Campbell, 2003]. However, a complex matrix representation of the polynomials [Lundstrom et al., 2007] enables scaling, rotation, translation and the transformation of elliptic pupil areas in one formalism.

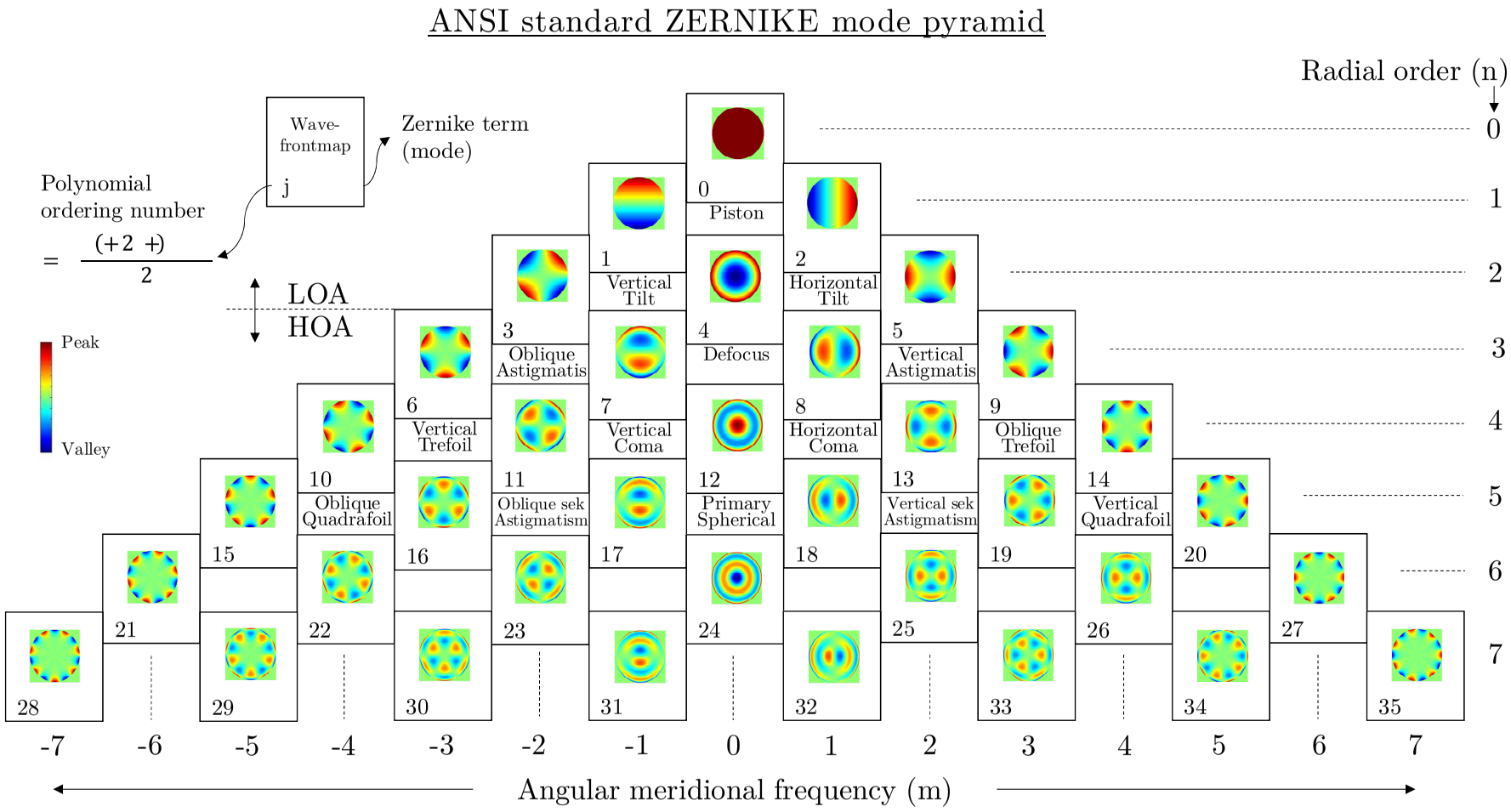

Figure 3: Table of Zernike base functions $Z_n^m(\rho, \theta)$ and their description in terms of Seidel aberrations. The weighted sum of these polynomials by the coefficient c_n^m can be used to define the actual shape of a wavefront for an individual eye. LOA = lower order aberrations describing terms with a radial order from n = 0 to n = 2 and HOA = higher order aberrations for terms with radial order n > 2.

1.2.3 Wavelength dependence of aberrations

Light as an electromagnetic wave interacts with matter depending on the energy of this wave. This interaction is described by the refractive index n. Light of shorter wavelength is higher in energy than light of longer wavelengths and therefore the refractive index $n(\lambda)$ is a function of the wavelength λ. The properties of aberrations described in the previous sections depend on the wavelength of light since the wave number $k = 2\pi/\lambda$ is calculated from λ. The differences in optical focusing error between different wavelengths is referred to as chromatic aberration. The longitudinal chromatic aberration (LCA) is defined as the variation of the focal length with the wavelength and even occurs for on-axis object points. The LCA of the eye shows a non-linear increase of refractive error with increasing wavelength with a range of $\Delta R_x \approx 2.0\,\mathrm{D}$ for the visual range of wavelengths (380 nm to 780 nm [ISO 20473:2007, 2007; Bennett and Rabbetts, 1998]) and is in-focus for a wavelength of $\lambda = 589\,\mathrm{nm}$ [Marcos et al., 1999b; Thibos et al., 1991]. The effect of focal shift is caused by the optical dispersion of the refractive media of the eye. Since the luminance spectrum of the eye has its a maximum around 550 nm and lower sensitivity for red and blue light [Thibos et al., 1991; Bennett and Rabbetts, 1998; Atchison and Smith, 2000], the weighted impact of chromatic aberration on visual performance can be estimated from polychromatic MTF as equivalent to spherical defocus of 0.2 D [Thibos et al., 1991] and mainly leads to a reduction in contrast. The inter-individual variability of the LCA is considered to be low [Charman and Jennings, 1976; Rynders et al., 1998; Marcos et al., 1999b; Howarth and Bradley, 1986].

As the angle between object point and optical axis increases, chromatic aberration leads to angular differences between the wavelengths and further to differences in (chromatic) magnification ΔMag_{Chrom}, this is referred to as transverse chromatic aberration (TCA). The TCA is proportional to the LCA and moreover depends on the distance between pupil and the nodal point of the eye [Thibos et al., 1991]. Typical values for the human eye are low $\Delta Mag_{Chrom} < 1.0\,\%$ and are therefore considered to affect vision least, compared to the LCA [Thibos et al., 1991]. If external pupils are used to restrict the incoming light, the chromatic magnification can increase to considerable values.

1.3 The human visual system - From the image to perception

1.3.1 Hierarchical organization of visual perception

The above descriptions were focusing on the physical definition of the optics of the eye. By definition, they characterize the optical transformation of an object into an image, transporting information regarding all physical properties (e.g. contrast, color or depth etc.) to the retinal plane of the eye. The human retina consists of a network of different cell types preprocessing the visual input. In bright light conditions, defined for luminance conditions of $L > 1.0\,cd/m^2$ [Zele and Cao, 2015; CIE, 1994], vision is mediated by cones and in dim light, vision is driven by rods [Kandel et al., 2000]. The existence of two different kinds of photoreceptor cells and their functional specificity is known as the *duplicity theory of vision* [Schultze, 1866; Weale, 1961]. The photochemical process of the conversion from light to neuronal electrical signals that takes place in the outer segment of the photoreceptors, is called visual phototransduction. It was first described by George Wald who also received the Nobel Prize for his discovery in 1967 [Wald, 1968].

The visual system of humans is a complex organization of different processing states starting with the optical properties of the eye's components, the retinal circuit incorporating the photoreceptors, bipolar and ganglion cells for the basic image processing, continued by the visual pathway. In the optic chiasma, the visual information from both eyes is separated into the same hemispheric visual field locations [Kandel et al., 2000]. Visual information originating from the left hemifield is projected to the rigth optic tract and further to the pretectum, where the control of pupil reflex takes place, to the superior colliculus, responsible for the processing of multisensory input and to the lateral geniculate nucleus. The complexity of the visual input, like color, depth, orientation, etc., is processed in higher cortical areas by feature extraction [Treisman, 1986] and reassembled in a detailed analysis depending on focused attention [Evans and Treisman, 2005]. The separation in feature based processing of visual information begins already in the retina, where two different types of ganglion cells project to the parvo- and magno-cellular layers of the LGN. These separation, called the "What" and "Where" organization [Mishkin et al., 1983], continues to the dorsal pathway with V1, V2, MT and the posterior parietal cortex where mainly motion, depth and luminance contrast information is processed. Additionally, the ventral pathway with V1, V4 and the inferior temporal cortex processes features like color, contrast and form [Ungerleider and Haxby, 1994; Kandel et al., 2000].

1.3.2 Assessment of visual perception

To investigate visual perception, scientists have long been using psychophysical methods. First, described by Fechner [Fechner, 1860], psychophysics studies the relationship between a physical stimulus intensity, for the visual sense: light intensity, contrast, color, spatial or temporal difference in luminance etc., and the resulting sensation or perception [Gescheider, 1997]. In case of spatial variations of local luminance L of an stimulus, this is described as contrast C and for sinusoidal stimulus pattern like the Gabor Patch [Peli, 1997] defined by the equation from Michelson [Michelson, 1927] (Equation 6).

$$C = \frac{L_{max} - L_{min}}{L_{max} + L_{min}} \tag{6}$$

The reciprocal of the smallest visible contrast threshold as a function of the spatial frequency of such patterns is referred to as the contrast sensitivity function (CSF). The curve describes the visual system as a bandpass filter with highest sensitivity around 4.0 cycles per degree (cpd) [Campbell and Robson, 1968]. The typical shape of the CSF (see Fig. 4a) is determined for the lower spatial frequencies by the lateral inhibition [Schade, 1956; Enroth-Cugell and Robson, 1966] of the retinal neuronal network and the drop at higher spatial frequencies is caused by the limited transfer ability of the optical components [Campbell and Green, 1965] of the eye. [Kelly, 1973; Barten, 1999] The cut-off frequency of the CSF, describing the highest frequency at which a contrast of $C > 0.99$ can still be perceived, is referred to as the resolution limit, namely the visual acuity of the eye.

To reliably and effectively assess the subjective CSF, psychophysical staircase methods are used [Kingdom and Prins, 2010]. On the basis of the forced-choice paradigm [Fechner, 1860] perceptual response to contrast stimuli below and above the threshold level are collected and the actual threshold is calculated as the contrast level at which 50 % of the stimuli were perceived correctly. Modern techniques for the assessment of the entire CSF ranging at spatial frequencies from SF = 0.5 cpd to SF = 60 cpd, are using computer-based estimations of threshold probability density [Lesmes et al., 2010; Gu et al., 2016] or variations in the stimulus presentation in combination with portable tablet computer devices [Dorr et al., 2013, 2017]. The assessment of the spatial contrast resolution properties of the visual system is used for instance for clinical diagnosis of age-dependent macular degeneration [Kleiner et al., 1988], Parkinson's disease [Bodis-Wollner et al., 1987] or dyslexia [Cornelissen et al., 1995; Stuart et al., 2001]. Regarding the impact of optics, the effect of induced spherical defocus on the contrast

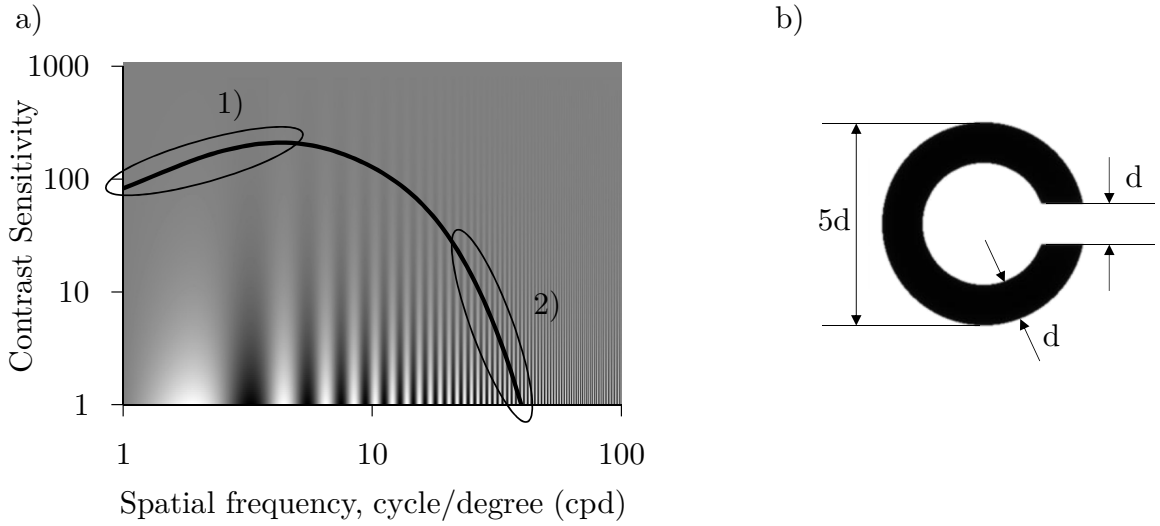

Figure 4: a) Schematic drawing of a typical contrast sensitivity function (black solid line) of the human eye superimposed by the Campbell & Robson contrast chart [Campbell and Robson, 1968], showing an increase of spatial frequency from left to right and a decrease of contrast from bottom to top. Contrast vision in part 1) of the function is limited by neural mechanisms, whereas the limitation in part 2) originates from the optics of the eye. b) Shows the Landolt C, the standard optotype for visual acuity testing. The smallest detail, the gap of the ring, is defined as 1/5 of the entire diameter.

sensitivity function was shown to be well predictable by the optical characteristics of the eye [Atchison et al., 1998] and therefore investigations on the CSF can further be used to understand the effect of optical correction on vision (e.g. optical designs of IOL [Montés-Micó and Alió, 2003; Bellucci et al., 2005] or contact lenses [Collins et al., 1989; Wahl et al., 2017]).

Additionally, an estimation of the resolution power of an optical system like the eye can provide a good measure of optical quality. Psychophysically, the visual acuity (VA) can be measured as the reciprocal of the smallest visual angle of two just separable adjacent points [Benjamin, 2006] and is typically expressed as the logarithm of the minimum angle of resolution, abbreviated by *logMAR*, in minutes of arc. Standard assessment procedures uses staircase algorithms like BestPEST [Lieberman and Pentland, 1982] in combination with a high-contrast ring pattern incorporating a defined gap [Bach, 1996], called the Landolt C [ISO 8596:2017, 2017], see Fig 4b. Since the visual acuity provides the maximum spatial frequency that is resolved by the eye, the relation between spatial frequency f_m and visual acuity is described by $f_m = 30 \,/\, \mathrm{VA(MAR)}$ [Artal, 2017].

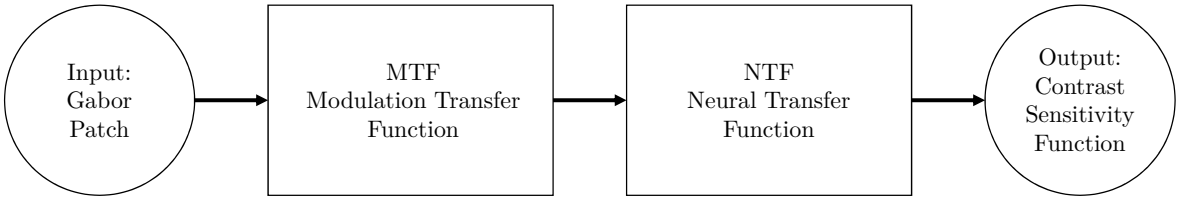

Figure 5: Simplified model to describe the contrast sensitivity function of the human eye as a response on an input that is filtered by the optical modulation transfer function and the neural transfer function. Both, the MTF and the NTF, are non-linear functions.

In addition to the clinical assessment of VA, the optical part of image degradation can be simulated on the basis of Fourier transforms. Legras et al. (2004) described an image simulation method that incorporates next to the optics of an optical lens the optical characteristics of the observer eye [Legras et al., 2004]. Simulated visual acuity was shown to result in similar results as lens-induced blur [Dehnert et al., 2011; Ohlendorf et al., 2011].

1.4 Image quality metrics in vision science

The *goodness* or perceived quality of an image by the visual systems depends on both, the optical quality and the neural processing. Since optical quality and the impact of different monochromatic and chromatic aberrations is described by metrics like the $PSF\,(x, y)$ or the $OTF\,(f_x, f_y)$, the characterization of the neural transfer function (NTF) is more challenging. The results of psychophysical measurements for instance the assessment of the lowest detectable contrast of a sinusoidal grating incorporating different spatial frequencies, can be used as perceptual measure of image quality. The contrast sensitivity function (CSF) is a composite of the two independent functions, the modulation transfer function and the neural transfer function (see Figure 5) and could therefore be used as an indirect measure to assess the NTF. Campbell & Green (1965) used a sinusoidal interference pattern that was projected on to the retina to directly measure the NTF for the smallest detectable contrast at different spatial frequencies by-passing the influence of the optics [Campbell and Green, 1965]. The technological development of adaptive optical systems enables researchers to correct monochromatic optical aberrations in a closed loop [Fernández et al., 2001; Marcos et al., 2017] and the NTF can be assessed [Williams et al., 2000; de Gracia et al., 2011] in a broader range of experimental parameters like for example for neural adaption to aberrations [Artal et al., 2004].

Image quality metrics are suggested to provide a numerical value as a measure of the goodness of the perceived image. They are based on the conjunction of optical

and neural transfer functions. Barten (1990) introduced an image quality metric called Square root integral, which uses the linear relationship between image quality and just-noticeable differences [Barten, 1990]. This metric was developed for the judgment of perceived image quality of television systems and is therefore restricted to spatial frequencies that are contributing to such systems. Later, Thibos et al. (2004) used a more general approach to precisely and accurately predict subjective refraction [Thibos et al., 2004]. They developed 33 image quality metrics classified in wavefront-based, PSF-based and OTF-based metrics. The visual Strehl derived from the optical transfer function, abbreviated by VSOTF, which is an area-based metric compromising optical intensity and phase changes weighted by the NTF [Campbell and Green, 1965], was shown to provide good accuracy and superior precision in predicting the spherical equivalent error [Thibos et al., 2004; Cheng et al., 2003; Leube et al., 2016c]. The formulas to calculate visual Strehl metrics are discussed in more detail in chapter 4 of the thesis. In addition to the evaluation of image quality of displays and the prediction of subjective refractive errors, numerical image quality estimations can be used to investigate the objective impact of aberrations on vision using through-focus curves. The range of defocus errors that degrade the visual Strehl value to a certain level is referred to a theoretical estimation of the depth of focus (DoF) [Yi et al., 2010]. However, comparisons of objectively determined DoF to the subjectively assessed DoF revealed no significant differences between mean values, but low correlations between single measures [Leube et al., 2015]. Besides the calculation of image quality, the retinal image of a point source can indirectly be recorded as a function of defocus by the use of double pass technique [Marcos et al., 1999b]. However, correlation of objective assessed DoF using this double pass imaging to subjective measures did not allow a simple translation because of non-linearities in their pupil size dependency.

Visual Strehl metrics like the VSOTF are described using monochromatic ocular aberrations. The calculation of the polychromatic point spread function $PSF_{poly}(x, y)$ can be achieved by summing up the single monochromatic PSF calculated for the given wavelengths and weighting by the source luminance spectrum $S(\lambda)$, see equation 7 [Ravikumar et al., 2008]. Similar concept can be applied to calculate polychromatic optical transfer function $OTF_{poly}(x, y)$. Calculations of TF-curves from polychromatic PSF and OTF showed a systematic increase in the estimated depth of focus [Ravikumar et al., 2008] which is supported by psychophysical results [Marcos et al., 1999b].

$$PSF_{poly}(x, y) = \int S(\lambda)\, PSF(x, y, \lambda)\, d\lambda \tag{7}$$

1.5 Perceptual depth of focus

The depth of focus of the eye, being described as "greatest range of dioptric focusing error which does not result in objectionable deterioration in the retinal image quality" [Atchison et al., 1997], depends on the perceptual judgment of the "objectionable deterioration" that is usually assessed by psychophysical methods. Classical experiments assessed the perceivable change in image quality by moving an object [Campbell, 1957] (or changing the angular size [Ogle and Schwartz, 1959]) in front of the eye, until it was perceived blurry. The corresponding axial changes in object related quantities is referred to as the depth of field, whereas the term depth of focus describes the image related quantities [Cline et al., 1997]. The depth of focus strongly depends on the pupil size, with a small pupil leading to a large DoF and a higher value in pupil size to a lower DoF [Marcos et al., 1999b; Ogle and Schwartz, 1959]. In very large pupil diameters, the subjective DoF is increasing again, mainly because of the increase in aberrations [Marcos et al., 1999b].

Subjective methods to assess the perceptual depth of focus further depend on a reliable definition of objectionable image deterioration that is commonly referred to a "just noticeable" blurring of the image [Atchison et al., 1997]. Atchison et al. (2005) investigated the influence of three different threshold criteria by introducing the terms *noticeable, troublesome* and *objectionable* blur limits [Atchison et al., 2005]. Results, obtained using a Badal-System [Atchison et al., 1995], and a high-contrast letter with angular size of 0.0 logMAR showed that regarding the noticeable criteria, the subjective DoF was $\pm 0.3\,\mathrm{D}$, while troublesome and objectionable limits were increased by a factor 1.6-1.8 and 2.1-2.5, respectively [Atchison et al., 2005].

In addition to the use of a sharp threshold, Legras et al. (2012) introduced a grading method based on calculated images from optical, monochromatic aberrations [Legras et al., 2012; Legras and Benard, 2013]. This method incorporates an image of letters beings blurred by convolution with the $PSF\,(x, y)$ for a range of optical aberrations are to be investigated. The participant have to grade the different images based on a 0 - 5 scale from excellent to bad [Legras and Benard, 2013]. This method has the further advantage that the influence of higher order aberration on the subjective image quality can be studied without the need of an adaptive optics system. However, simulated images are limited in the change of intensity ($MTF\,(f_x, f_y)$) and not in phase ($PTF\,(f_x, f_y)$), like real aberrations would impose as well.

2 Objectives

The depth of focus is an important property of the human visual system and is therefore of high interest for the development of novel correction techniques of refractive errors, like spectacle lenses, contact and intraocular lenses and refractive surgeries. Studies analyzing the influence of higher order aberrations such as spherical aberration or coma on the depth of focus showed that optical aberration can be used to enhance the depth of focus [Benard et al., 2011; Rocha et al., 2009]. However, higher order aberrations are defined for the static position of the eye, optically defined as the position of the exit pupil, regarding the correction, which is not the case for spectacle lenses. The purpose of the first described project was to investigate the influence of induced primary astigmatism, a type of lower order aberration, on the subjective depth of focus. The presented results could be used to develop novel optical lenses for the correction of presbyopia.

Since the human visual system is adapted to the inherent optical aberrations [Artal et al., 2004], the correction or even a change of aberrations leads to discomfort in the visual experience. Therefore, the knowledge of individual depth of focus and the impact of different types of aberrations on the blur perception could improve the optimization process of optical corrections. The aim of the second project was to investigate the effect of individual neural transfer functions on the agreement between objective and subjective depth of focus. The obtained results could lead to further developments in individualized prediction for optical correction and could improve their compliance.

Psychophysical measurements under polychromatic white light conditions (part of the first project) revealed that the perceptual sensitivity to induced spherical defocus depends on the sign of defocus [Radhakrishnan et al., 2004b; Leube et al., 2016b]. In addition to the implications towards a deeper understanding of the emmetropization process of the eye, this phenomena have a high relevance for the assessment of through-focus curves to investigate the goodness and the depth of focus of mono- and multifocal optical corrections, like IOL's. The objective of the third project of this thesis was to investigate two possible causes of the asymmetric reduction of visual performance for sign-different induced spherical defocus: polychromaticity and light's vergence. Assessment of visual acuity under monochromatic light conditions with lens-induced and image-simulated blur conditions were investigated.

3 Subjective depth of focus and induced astigmatic aberration

Leube, A., Ohlendorf, A., & Wahl, S. (2016). The Influence of Induced Astigmatism on the Depth of Focus. Optometry and Vision Science, 93(10), 1228-1234. doi:10.1097/OPX.0000000000000961

3.1 Abstract

Purpose: To evaluate whether an induced astigmatism influences the subjective depth of focus.

Methods: 51 participants aged 18 - 35 years and with a mean spherical equivalent refractive error of 0.51 ± 2.35 DS participated in the study. The accommodation was blocked with three drops of 1 % Cyclopentolate. Refractive errors were corrected after subjective refraction with a 4 mm artificial pupil. To evaluate the depth of focus (DoF), defocus curves with a spherical range of ± 1.5 DS were assessed. The DoF was calculated as the horizontal distance at a threshold level of $+0.1$ logMAR from the maximum visual acuity (VA). Defocus curves were estimated binocularly during distance (500 cm) and a near vision (40 cm) for two induced axis (ATR in 0° and WTR in 90°) and for a fixed amount of astigmatic defocus of - 0.5 DC.

Results: The mean natural DoF was 0.885 ± 0.316 D for far vision and 0.940 ± 0.400 D for near vision. With induced astigmatism the DoF for far vision was significantly increased to 1.095 ± 0.421 D ($p = 0.006$, ANOVA) for the WTR astigmatism but not for the ATR astigmatism (1.030 ± 0.395 D; $p = 0.164$, ANOVA). The induced WTR astigmatism enhanced the DoF for near vision significantly to 1.144 ± 0.338 D ($p = 0.04$, ANOVA), DoF with induced ATR astigmatism (0.953 ± 0.318 D) was not significantly different ($p = 1.00$, ANOVA). ATR-astigmatism reduced VA by $+0.08 \pm 0.08$ logMAR ($p < 0.01$, t-Test).

Conclusion: With an induced WTR astigmatism of - 0.5 DC, the DoF can be enhanced in the near viewing distance with a marginal loss in binocular VA. The approach of using induced simple WTR astigmatism can lead to novel optical treatments for presbyopia.

3.2 Introduction

The depth of focus (DoF) of an eye is defined as the "greatest range of dioptric focusing error which does not result in objectionable deterioration in the retinal image quality" [Atchison et al., 1997]. Different methods were developed to measure the subjective as well as the objective depth of focus of the human eye [Atchison et al., 2005; Marcos et al., 1999b; Vasudevan et al., 2006; Yi et al., 2010]. All measurements suffer from the

challenge of exactly defining the deterioration that objectionably reduces the retinal image quality. For subjective methods, Atchison et al. defined limits for the visual perception of noticeable, troublesome and objectionable blur [Atchison et al., 2005]. Other authors used a range of induced defocus which decreases the visual performance, e.g., visual acuity or contrast sensitivity, below a certain threshold to calculate the depth of focus from the obtained defocus curves [Ogle and Schwartz, 1959; Legge et al., 1987; Nio et al., 2000; Green et al., 1980]. The method to determine the depth of focus out of objective measurements is similar. Objective performance values, e.g., image quality metrics (IQM) or double pass images (DPI) in the retina plane, can be achieved over a certain range of defocus. [Marcos et al., 1999b; Yi et al., 2010; Green et al., 1980] The depth of focus is then calculated as the dioptric range at a fixed threshold level (e.g., Hopkins criterion [Marcos et al., 1999b] or 50 % of the peak value [Legge et al., 1987]). Objective depth of focus can be also assessed by measuring the smallest amount of change of an accommodative stimulus that causes a detectable change in the accommodative response [Vasudevan et al., 2006; Yao et al., 2010].

The most prevalent solution to correct presbyopia is the use of progressive spectacles lenses, which restore far and near vision in a single lens without loss in visual acuity for intermediate distances. The spherical power of a progressive addition lens (PAL) increases along a vertical line and is in the periphery surrounded by astigmatic errors [Sheedy et al., 2005]. These lateral deteriorating errors restrict the comfortable dynamic vision for intermediate and near distances of the wearer. Other multifocal corrections for presbyopia, e.g., multifocal contact lenses or intraocular lenses, generate acceptable far and near vision by producing simultaneous foci in the retina plane. As a main consequence, the contrast sensitivity is decreased and some wearers report halo effects [Pieh et al., 2001]. From subjectively measured defocus curves, it is known that these types of corrections of presbyopia enhance the depth of focus. [Artal et al., 1995; Schmidinger et al., 2006] Therefore, these optical solutions can also be used to correct vision over a large range of viewing distances. Different optical approaches were developed to enhance the natural depth of focus, mainly with higher order aberrations by the use of adaptive wavefront optic systems. Especially spherical aberration can increase the natural DoF by 2.0 D ($Z(4,0)$ of $+6.0\,\mu m$) [Rocha et al., 2009] or by 0.8 D with a combination of primary $Z(4,0)$ of $+6.0\,\mu m$ and secondary $Z(6,0)$ of $+0.25\,\mu m$ spherical aberration [Yi et al., 2011]. Nevertheless, it is difficult to incorporate these approaches into current optical designs of progressive addition lenses (PAL), because higher order aberrations (HOA) are always gaze angle-dependent and their amplitude differs with the gaze position. However, lower order aberrations (LOA), like defocus and primary astigmatism, do not show this dependency and it was reported

that against-the-rule astigmatism can be beneficial in near vision [Nagpal et al., 2000; Trindade et al., 1997; Hayashi et al., 2000]. Huber showed that eyes with implanted IOL and a postoperative simple myopic astigmatism had an quasi-constant visual acuity over different distances [Huber, 1981b,a] and he concluded that this astigmatism might increase the depth of focus. However, Huber did not analyze the depth of focus explicitly. In the Myopic Astigmatism and Presbyopia Trial, Savage and colleagues conducted a study on the influence of low astigmatic refractive errors regarding the visual acuity, stereopsis and quality of life of presbyopia patients [Savage et al., 2003] They stated that, theoretically, low astigmatism improves the depth of focus, but they did not perform direct measurements of the depth of focus in the different astigmatic conditions. Nevertheless, it is well known that the easiest method to enhance the depth of focus of an eye is to induce defocus - either spherical, astigmatic or using higher order aberrations. That reduces the threshold visual acuity with the consequence of an enhanced depth of focus for the eye. Therefore, the purpose of this study was to evaluate whether induced astigmatism can enhance the subjective depth of focus of the human eye in far and near vision without a noticeable reduction of the visual acuity.

3.3 Methods

3.3.1 Study protocol

A prospective, controlled study was carried out at the University of Tuebingen with 51 eye-healthy subject aged 18 to 35 years. The mean spherical equivalent refractive error (SE) was $0.51 \pm 2.35\,\mathrm{D}$ in the right and $0.66 \pm 2.22\,\mathrm{D}$ in the left eye. Inclusion criteria were a visual acuity higher than 0.0 logMAR and no known eye diseases. Subjects with ametropia higher than $\pm 6.0\,\mathrm{DS}$ and $\pm 2.0\,\mathrm{DC}$, allergy to Cyclopentolate Hydrochloride or contradictions to mydriasis were excluded. All participants had a full ophthalmic examination as well as an objective and subjective refraction to correct habitual refractive errors of the eye. Prior to mydriasis, the intraocular pressure, the anterior chamber angle and the pupils light reaction were checked by an ophthalmologist. The pupil dilatation and accommodation paralysis were achieved using three drops of a cycloplegic agent (1 % Cyclopentolate Hydrochloride, Alcon Ophthalmika GmbH, Austria) with ten minutes in between of every application prior to the experiment. There was also a break of 10 min between the last drop and the beginning of the study measurements. Three measurements of the objective refraction and the pupil diameter were performed, using a wavefront aberrometer (ZEISS i.Profiler plus, Carl Zeiss Vision GmbH, Germany). The most positive reading of the objective refraction (for the spherical refractive error) was used as starting value for the subjective refraction. A trial frame (UB4, Oculus, Germany) and trial lenses with an artificial pupil

of 4 mm diameter in a photopic environment (L = 250 cd/m^2) were used to achieve the optimal subjective refraction in a distance of 5 m. End point of monocular refraction was the maximum plus power with highest visual acuity. The visual acuity was measured according to the standard DIN EN ISO 8597 with SLOAN-Letters. Both, objective and subjective refraction were obtained after installing the cycloplegic agent to account for latent hyperopia. To ensure that the cycloplegic effect was fully emerged, three push-up measurements from first clear to first noticeable blur in the distal and proximal direction were performed before, in between and after the course of the experiment [Chen and O'Leary, 1998]. A row of five SLOAN letters with an angular size of 0.0 logMAR, presented on an OLED Display, was used as the test chart. To achieve a non-blurred near vision for the 40 cm viewing distance, the spherical component of the distance refraction was shifted by + 2.50 DS. Subjects with an accommodation range higher than 1 D after cycloplegia were excluded from the analysis.

The study followed the tenets of the Declaration of Helsinki and was approved by the Institutional Review Board of the medical faculty of the University of Tuebingen. Informed Consent was obtained from all participants after the content and possible consequences of the study had been explained.

3.3.2 Subjective measurements

The depth of focus (DoF) was measured under three different conditions in two different viewing distances. DoF was assessed for the best subjective correction and with additionally induced negative astigmatism of - 0.5 DC. Adding this lens in an axis of 180° (or 0°), it will induce an ATR astigmatism, while it will induce WTR astigmatism, when the lens is placed in 90°. These three conditions were tested for far vision in 500 cm and for near vision in 40 cm viewing distance with a vertex distance of 12 mm. The induced astigmatism was combined with the subjective refraction to a resulting sphero-cylindric power in order to keep a constant number of trial lenses during the experiment (two lenses, sphere and cylinder) [Raasch, 1995]. The combination of two or more different sphero-cylindrical corrections is based on the vector analysis of refractive errors using Fourier decomposition [Thibos et al., 1997]. The principal components M, J_0 and J_{45} were added and the resulting correction was converted back to the conventional notation of sphere, cylinder and axis. For the near vision testing, the spherical correction was shifted for + 2.5 DS to compensate the blocked accommodation of the eyes. Measurement sequence was randomized according to viewing distance and the axis of the induced astigmatism. All recordings were done binocularly and with artificial pupils of 4 mm diameter. The FrACT, a psychophysical, adaptive staircase procedure (Freiburg Visual Acuity Test [Bach, 1996], Best PEST fitting method) was used to measure the

visual acuity as a function of induced spherical defocus with a range of ± 1.5 DS in 0.5 DS steps. High contrast Landolt C's were used as optotypes, with eight possible gap directions. To reduce the variability of the measured visual acuity, [Bach, 2007] one psychophysical staircase procedure consisted of 24 presentations of the Landolt C. The visual acuity was measured in focus as well as in defocused conditions and all three refractive conditions were performed in the two viewing distances. A LED monitor (UltraSharp U 2321H, Dell Inc., Round Rock Texas, USA) and an OLED monitor (SVGA+, eMAgin Corp., Bellevue, USA) were used for far and near vision testing, respectively, both with a minimum luminance of $\mathrm{L} = 200\, cd/m^2$.

3.3.3 Threshold definition and analysis of defocus curves

The method to calculate the depth of focus from a defocus curve was adapted from Schwarz et al. [Schwarz et al., 2012].In the current study, the DoF is defined as the horizontal dioptric range at the threshold level of +0.1 logMAR below the maximum value of visual acuity. Using this method, the depth of focus is analyzed for a high visual acuity threshold and it can be ensured that the different refractive conditions are comparable by the normalization to the maximum. The threshold definition with a relatively small reduction of the visual acuity (0.1 logMAR is equivalent to one line in an acuity chart) was chosen because a greater drop of the visual acuity would probably not be accepted by the wearer. The calculation of depth of focus from the obtained defocus curves is illustrated in Figure 6. Pairs of consecutive visual acuities were identified such that the position of the threshold function is within these acuity points. The depth of focus was calculated as the absolute distance under the defocus curve. These calculations were done using Matlab (Matlab 2014a, MathWorks Inc., Natick, USA). For every viewing distance, the depth of focus was calculated for the following conditions:

1. Best subjective correction
2. Combined correction: best subjective correction + induced astigmatism of -0.5 DC $0°$
3. Combined correction: best subjective correction + induced astigmatism of -0.5 DC $90°$

Depth of focus data were analyzed using a statistics program (SPSS v.22.0, IBM Corp., Armonk, USA). Normality of data distribution was assessed by the Shapiro-Wilk test. A one-way ANOVA and a post hoc test (α correction by using the Bonferroni method) were applied to test for differences between the best correction status and the induced astigmatisms for the two viewing distances. Differences were considered to be

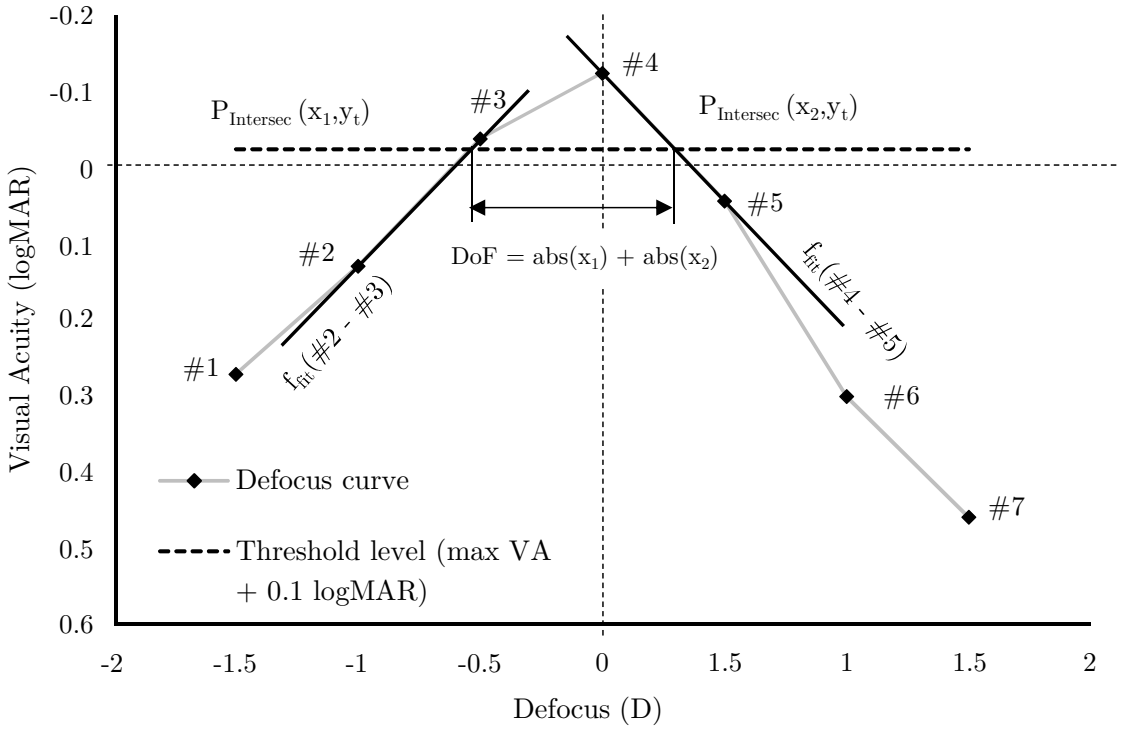

Figure 6: Example defocus curve (full corrected subject) and illustration of the calculation of the depth of focus. Measured visual acuity points are represented by indices from #1 to #7. To calculate the depth of focus, two pairs of consecutive indices of acuities (#2, #3) and (#4, #5) were identified such that the elements of the pairs have opposite signs in the difference between the measured acuity and the threshold acuity ($VA_{\#2} - VA_t$, $VA_{\#3} - VA_t$). The depth of focus (DoF) in diopters is defined as the distance between the two intersection points $P_{intersec}$ (x_1,y_t) and $P_{intersec}$ (x_2, y_t) of the linear functions $f_{fit}(\#2 - \#3)$ and $f_{fit}(\#4 - \#5)$ and the threshold function ($y_t = VA_t = VA_{max} + 0.1$).

statistically significant when the p-value was $\alpha < 0.05$. The required sample size was calculated for all three conditions with a statistical power analyzer (G*Power 3.1.9.2, Franz Faul, University Kiel, Germany, [Faul et al., 2007]) and the following parameters: $\alpha = 0.05$, $1 - \beta = 0.85$, $\Delta\mu = 0.18$ D, $\Delta\sigma = 0.40$ D, paired t-test for one sample. The calculation resulted in a requirement of at least $n = 48$ subjects.

3.4 Results

3.4.1 Residual accommodation and pupil diameter

The residual range of accommodation was calculated as the average of the results from the distal and proximal push-up measurement [Chen and O'Leary, 1998]. The average residual accommodation after cycloplegia was 0.32 ± 0.22 D and there was no significant change during the time course of the experiment ($p > 0.05$, t-Test). The mean pupil diameter after the full cycloplegic effect was emerged, was 5.97 ± 0.87 mm and did not change over the study time ($p > 0.05$, t-Test). To evaluate the effect of the residual accommodation on the depth of focus, correlation analysis were performed. There was no significant correlation between the residual accommodation and the measured depth of focus for the far ($r = 0.082$, $p = 0.567$, Pearson) or the near ($r = -0.132$, $p = 0.355$, Pearson) viewing condition found.

3.4.2 Depth of focus with induced astigmatism

For the measurement distance of 5 m, the obtained results of one subject had to be excluded because the visual acuity was higher than the threshold level in all negative defocus steps. For the remaining 50 subjects, the natural depth of focus of the study group ranged from 0.455 D to 2.083 D with a mean value of 0.885 ± 0.316 D. Subgroup-analysis of the axis of the inherent astigmatism regarding the natural depth of focus was performed with grouped results according classification by orientation of astigmatism from Benjamin: with-the-rule (axis $0° \;\&\; 180° \pm 20°$), against-the-rule (axis $90° \pm 20°$) and oblique astigmatism [Benjamin, 2006]. There was no difference in the natural depth of focus within the groups, not for the far viewing ($F(2,46) = 0.987$, $p = 0.380$, ANOVA) nor for the near viewing condition ($F(2,46) = 1.095$, $p = 0.343$, ANOVA).

Compared to the depth of focus measured without induced astigmatism (see Figure 7), there was a significant enhancement of the DoF with the induced WTR astigmatism to 1.095 ± 0.421 D ($\Delta\, DoF_{WTR} = 0.210$ D; $F(2,147) = 5.09$, $p = 0.006$) but no significant difference was observed, when the ATR astigmatism was induced (DoF_{ATR}: 1.030 ± 0.396 D; $\Delta\, DoF_{ATR} = 0.145$ D; $F(2,147) = 5.09$, $p = 0.164$). The mean DoF without induced astigmatism during near vision (see Figure 8) was 0.940 ± 0.400 D

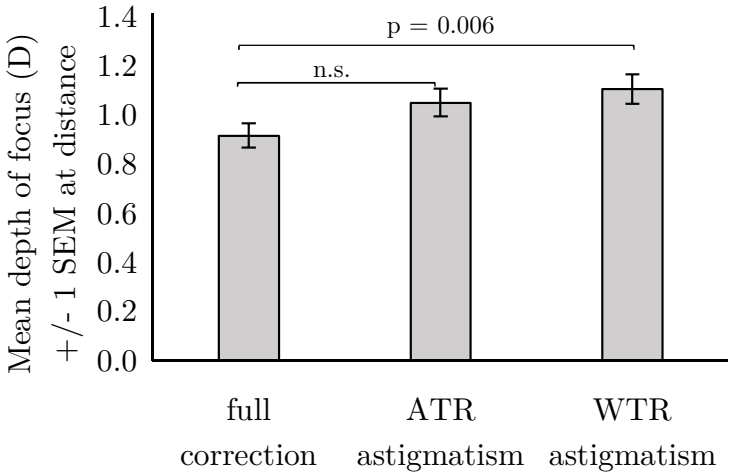

Figure 7: Mean depth of focus [D] with full correction and with induced ATR and WTR astigmatism for far (500 cm). Error bars represent ± 1 standard error of the mean (SEM).

(range 0.336 to 2.215 D). It was significantly enhanced with the induced WTR astigmatism to an average of 1.144 ± 0.338 D ($\Delta DoF_{WTR} = 0.200$; F (2,150) = 4.352, p = 0.04). The DoF with induced ATR astigmatism lacked a significant change compared to the natural depth of focus (0.953 ± 0.318 D, $\Delta\, DoF_{ATR} = 0.013$ D; F (2,150) = 4.352, p = 1.00). The differences in the enhancement of the depth of focus between the two axes of induced astigmatism is statistically significant, but lacks clinical relevance. Subgroup-analysis of the increase of depth of focus regarding the type of the habitual astigmatic correction was performed without resulting in a significant difference between the groups for both viewing conditions (Far: F (2,47) = 1.024, p = 0.367, ANOVA; Near: F (2,48) = 0.555, p = 0.578, ANOVA).

With the induced astigmatism, the visual acuity in the far viewing distance was significantly reduced by 0.05 ± 0.07 logMAR ($p < 0.01$, t-Test) and by 0.08 ± 0.08 logMAR ($p < 0.01$, t-Test) for the ATR and WTR astigmatism, respectively. For the near viewing distance, the reduction was 0.03 ± 0.10 logMAR (p = 0.056, t-Test) and 0.07 ± 0.07 logMAR ($p < 0.01$, t-Test) for the ATR and WTR astigmatism, respectively. As one could expect, highly significant correlations ($p < 0.001$, Pearson) were found for the enhancement in the depth of focus and the decrease in visual acuity. Correlations were found for all axis and all viewings distances. A subgroup analysis showed that there was no difference in natural depth of focus between myopic (n = 29) and non-myopic subjects for far vision (p = 0.337, paired t-Test, n = 22) and near vision (p = 0.533, paired t-Test). The enhancement of the depth of focus with an induced WTR astigmatism for far and near vision was greater in myopic subjects

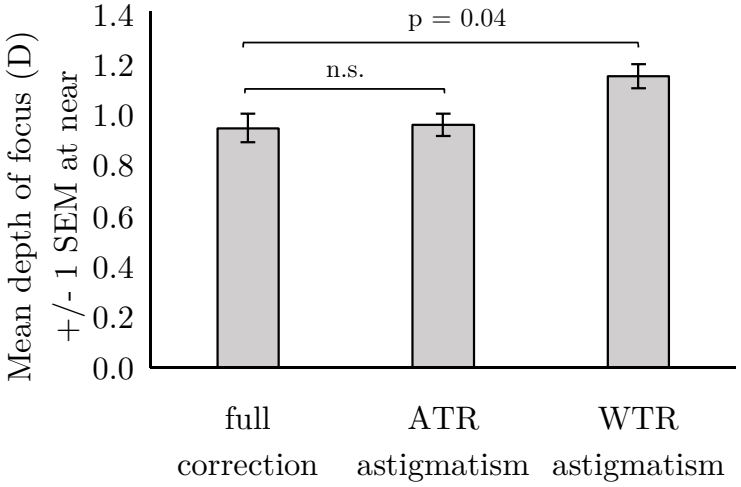

Figure 8: Mean depth of focus [D] with full correction and with induced ATR and WTR astigmatism for near (40 cm). Error bars represent ± 1 standard error of the mean (SEM).

($\Delta\, DoF_{Far} = 0.16\,\mathrm{D}$, $p_{Far} = 0.016$; $\Delta\, DoF_{Near} = 0.20\,\mathrm{D}$, $p_{Near} = 0.010$, paired t-Test) compared to the non-myopic subjects (induced WTR astigmatism: $\Delta\, DoF_{Far} = 0.19\,\mathrm{D}$, $p_{Far} = 0.081$; $\Delta\, DoF_{Near} = 0.12\,\mathrm{D}$, $p_{Near} = 0.112$, paired t-Test), but the results lacked statistical significance. On the other hand, a larger enhancement of the depth of focus for far vision with the induced ATR astigmatism was found in non-myopic subjects ($\Delta\, DoF_{Far} = 0.16\,\mathrm{D}$, $p_{Far} = 0.032$, paired t-Test) compared to myopes ($\Delta\, DoF_{Far} = 0.09\,\mathrm{D}$, $p_{Far} = 0.346$, paired t-Test).

3.5 Discussion

3.5.1 Depth of focus with induced astigmatism

Several methods with the attempt to enhance the depth of focus of the human eye by inducing optical errors using several types of aberrations were published previously [Rocha et al., 2009; Huber, 1981b,a; Rocha et al., 2007; Benard et al., 2011, 2010]. In the present study, induced astigmatism of 0.5 DC, without a spherical compensation, in the same horizontal or vertical orientations in both eyes, was used to test if small induced astigmatism could enhance the depth of focus of the eye. As a consequence, the spherical equivalent is not equivalent to zero and the circle of least confusion is not on the retina. This could result in a shift of the measured defocus curve towards hyperopia. To avoid misleading results out of this shift in the results of the calculated depth of focus, we used a threshold definition that was based on the maximum visual acuity and not on the zero defocus location. The results of our study showed that the depth of focus of the human eye can be significantly enhanced by on average 0.2 D with

an induced WTR astigmatism of - 0.5 DC, for both far and near viewing distance. In the presence of primary astigmatism, already published studies also indicate that the depth of focus can be enhanced including a benefit for near vision tasks. For example, Huber showed that eyes with implanted IOL and a planned postoperative simple myopic astigmatism have a "quasi-constant visual acuity over different distances" and he concluded that astigmatism increased the depth of focus [Huber, 1981b,a]. However, Huber did not analyze the depth of focus explicitly. Savage and colleagues performed a study that examined "whether low astigmatism benefits or harms patients with presbyopia, whose intermediate and near vision theoretically benefit from enhanced depth of focus provided by astigmatism" [Savage et al., 2003]. Nevertheless, the authors investigated the influence of astigmatism on the visual acuity, the near stereopsis and the quality of life - an analysis of the depth of focus was not conducted. Theoretical calculations of Sawusch et al. obtained an optimal depth of focus for a schematic eye model with a plus cylindrical component and an equaled negative sphere of - 0.25 DS and showed high correlations to subjective measurements [Sawusch and Guyton, 1991]. Kim et al. suggested that orthogonal orientations of astigmatic errors (one eye an induced ATR and the other eye a WTR astigmatism) resulted in better acuity, but they were not able to show significant differences [Kim et al., 2014]. The explanation of an enhanced DoF with induced primary astigmatism is the theory of Sturm's hypothesis. Concerning this theory, when there is a single point refracted through an astigmatic lens, the image are two focal lines, separated by a focal interval [Nagpal et al., 2000]. If this extension of the focal range does not result in objectionable deterioration in the retinal image quality (according to the definition of the depth of focus) [Atchison et al., 1997] this results in an increased depth of focus.

The benefit of an induced astigmatism for the near visual acuity is reported in many studies, mainly from research on intraocular lenses. Against-the-rule (ATR) myopic astigmatism seems to provide superior near visual performance compared to with-the-rule (WTR) astigmatism, resulting in higher near acuity and better near stereopsis [Nagpal et al., 2000; Hayashi et al., 2000; Savage et al., 2003]. Results of the current study showed a decrease in near visual acuity of 0.07 logMAR for induced WTR astigmatism and of 0.03 logMAR for induced ATR astigmatism. The decrease in far visual acuity was 0.08 logMAR for induced WTR astigmatism and 0.05 logMAR with induced ATR astigmatism. Because the induced WTR astigmatism resulted in a slightly higher reduction in visual acuity for far vision, which can result in a beneficial increase of the depth of focus. Nevertheless, the observed differences of 0.04 logMAR are not clinical relevant. Atchinson (2009) has shown that the effect of astigmatic defocus on optotyp recognition is dependent on the axis of the induced astigmatism, especially when closed

letters are used as optotypes [Atchison et al., 2009a]. One main difference of the current study to previously published ones [Nagpal et al., 2000; Savage et al., 2003] is that the Landolt C was used as an optotype, where the dependency of the optotype against the orientation of the blur limits is reduced. Since the induced astigmatism can change the spherical component of the correction of the habitual refractive error, different axes of induced astigmatism can further lead to different changes in the spherical power. To test if an induced astigmatism without a spherical compensation has an influence on the spherical equivalent component of the habitual refractive error, the spherical equivalent refractive error was compared for all defocus conditions. Statistical analysis revealed no significant difference between the habitual correction and the resulting corrections, with an induced ATR or WTR astigmatism for far vision ($p_{ATR} = 0.119$, $p_{WTR} = 0.214$) and for near vision ($p_{ATR} = 0.142$, $p_{WTR} = 0.220$). Therefore, the enhancement of the DoF cannot be explained by a spherical shift that is caused by the induced astigmatism. Furthermore, the magnitude of inherent astigmatism can be assumed to influence the subjective blur sensitivity. Vinas et al. found that astigmatic correction leads to a significant shift of the perception of the neutral point [Vinas et al., 2012]. In the current study, we did not found an influence of the amount of cylindrical ametropia on the natural DoF nor on the depth of focus measured with induced astigmatism ($r < 0.24$, $p > 0.05$, Pearson) for both viewing distances. There was also no significant difference found when the increase in depth of focus is compared within the groups of habitual astigmatic corrections. This rejects any subjective preferences based on the inherent ametropia of the patient.

Subjective measurements of defocus curves were performed under binocular conditions for distance (500 cm) and near vision (40 cm). To take into account the convergence that is needed during near vision, the subjects were instructed to adjust the artificial pupil such that the stimulus was centered in the visual field of each single eye as well as under binocular conditions, without moving the head. Since convergence is also driven by accommodation and the constriction of the pupil, we used a cycloplegic agent to control both cues. As mentioned before, the reduced pupillary distance during near vision was controlled by the rearrangement of the pupillary distance within the trial frame.

3.5.2 Limitations of the study

The present study was conducted with young subjects aged from 18 to 35 years. One limitation is that these subjects did not lack a natural loss of their accommodation compared to subjects aged 40 years and older. Even with dilated pupils and a strong cycloplegic effect that was achieved using 3 drops of 1 % Cycloplentolate Hydrochloride, we cannot assure that the measurements would be different if the same study course would have been realized with subjects aged 40 years and older. For example, it can be assumed that our young study group would exhibit higher values of residual accommodation even under cycloplegia, compared to older subjects, where a limited accommodative range in collaboration with a cycloplegic agent might result in an even smaller amount of residual accommodation. Additionally, one might speculate that the sensitivity to induced astigmatic blur changes with age, since it is known that there is a trend towards against-the-rule astigmatism with increasing age and this could result in less ATR-blur sensitivity in elderly people [Ferrer-Blasco et al., 2008]. Another influencing factor could be the change in the depth of focus of the eye with age. It was previously published that due to changes in the ocular aberrations of the eye and changes in the pupil diameter with age (natural miosis), the natural depth of focus of the eye increases by 0.027 D per year for subjects aged 20 to 50 years [Wang and Ciuffreda, 2006; Mordi and Ciuffreda, 1998]. Therefore, a transfer of the results to an older subject group have to be done carefully. We did not test different amounts of induced astigmatism or different combination of its axis in the both eyes, as suggested from Kim et al. [Kim et al., 2014]. To increase the accuracy of the defocus curve further studies could use increments of spherical defocus of 0.25 DS. On the other hand this enlarges the study time for the subject and can lead to fatigue effects, when visual acuity is measured.

3.6 Conclusion

The current study gave evidence for an enhancement of the depth of focus with an induced negative WTR astigmatism for both, the far and the near viewing distance with a marginal reduction in visual acuity. Further studies have to be carried out to test if an enhancement of the depth of focus using induced astigmatism can provide a better visual performance for the wearer of optical solutions that correct presbyopia.

Acknowledgements

This research received no specific grant from any funding agency in the public, commercial, or not-for-profit sectors. A. Leube, A. Ohlendorf and S. Wahl report no financial interests or potential conflicts of interest.

4 Neural transfer function and its influence on the prediction of subjective depth of focus

Leube, A., Schilling, T., Ohlendorf, A., Kern, D., Ochakovski, A. G., Fischer, M. D., & Wahl, S. (2018). Individual neural transfer function affects the prediction of subjective depth of focus. Scientific Reports, 8(1), 1919. doi:10.1038/s41598-018-20344-x

4.1 Abstract

Attempts to accurately predict the depth of focus (DoF) based on objective metrics have failed so far. We investigated the effect of the individual neural transfer function (iNTF) on the quality of the prediction of the subjective DoF from objective wavefront measures. Subjective DoF was assessed in 22 participants using subjective through focus curves of visual acuity (VA). Objective defocus curves were calculated for visual Strehl metrics of the optical (VSOTFa) and the modulation transfer function as well as the point spread function. DoF was computed for residual lower order aberrations (rLoA) and incorporation of iNTF. Correlations between subjective and objective DoF did not reach significance, when a) standard metrics were used and b) rLoA were considered ($r_{max} = 0.33$, $p_{all} > 0.05$). By incorporating the iNTF of the individuals in the calculation of the objective DoF from the VSOTFa metric, a moderate statistically significant correlation was found ($r = 0.43$, $p < 0.01$, Pearson). The iNTF of the individuals eye is fundamental for the prediction of subjective DoF using the VSOTFa metric. Individualized predictions could aid future application in the correction of refractive errors like presbyopia using intraocular lenses.

4.2 Introduction

The neural transfer function (NTF) is next to the optical transfer function (OTF) one part of the overall contrast sensitivity function of the human eye [Watson and Ahumada, 2008]. The assessment of the NTF requires to by-pass the optical part and to assess the perceptual part alone. Technically this can be achieved by using interference fringe technique [Campbell and Green, 1965; Dressler and Rassow, 1981]. While using this technique, a sinusoidal strip pattern is projected onto the retina that is not influenced by the optics of the eye. The contrast and the spatial frequency can be changed in a way that the neural part of the contrast perception (the neural transfer function) of the retina-brain-system, can be assessed separately from the characteristics of the optics. Using a second method, that measure the wavefront errors of an individual's eye, the neural part of the perception of contrast gratings can be calculated [Michael et al., 2011] out of the derived modulation transfer function (MTF) and

the contrast sensitivity function (CSF). The knowledge of the neural contrast transfer property of the human visual system is an important parameter since image quality depends on both, the optical and the neural factors of vision [Campbell and Green, 1965; Thibos et al., 2004; Barten, 1990, 1999]. Numerical expressions, the so called image quality metrics, consider both information, the objective measures of the optical quality and the psychophysically assessed neural perception function [Barten, 1999]. In 1987, Barten proposed a metric called square root integral (SQRI) that incorporated the neural threshold level of the human eye, with the aim to quantify the resolution visibility in displays [Barten, 1987]. Later, Thibos et al. described 33 image quality metrics and showed high precision of wavefront based metrics for the prediction of the subjective spherical equivalent error [Thibos et al., 2004].

Objective image quality metrics can also be used to calculate defocus curves and estimate the objective depth of focus at a defined threshold level [Yi et al., 2010]. So far, fixed threshold levels (for example 50 % [Jansonius and Kooijman, 1998; Legge et al., 1987] or 80 % [Marcos et al., 1999b]) from the maximum of the defocus curve or individual thresholds that are based on the root mean square of the amount of higher order aberrations [Yi et al., 2010], were used. The depth of focus of the eye is defined as "the greatest range of dioptric focusing error which does not result in objectionable deterioration in the retinal image quality" [Atchison et al., 1997]. This definition includes that the subjective and objective measures strongly depend on the definition of an "objectionable deterioration" of the retinal image. However, some studies [Benard et al., 2011; Legras et al., 2012] that tried to find good predictions of the subjective depth of focus calculated from image quality metrics failed. Nevertheless, the calculation of the depth of focus from objective through focus curve generated using image quality metrics is widely used for performance measure, for example of intraocular lenses [Artal et al., 1995; Baumeister et al., 2009; Prez-Merino et al., 2014] or to investigate the influence of aberrations on the visual performance of the eye, for example in form of the visual acuity [Xu et al., 2013; Marsack et al., 2004; Cheng et al., 2003]. One step further for the future of individualized biomedical applications is the use of personal data, such as the individual neural transfer function (iNTF).

Therefore, it was the aim of the current study to evaluate the influence of the iNTF and several confounding factors on the prediction of the subjective depth of focus from objective metrics.

4.3 Methods

4.3.1 Participants

Twenty eight young and eye healthy participants were enrolled in the study. Six participants had to be excluded from the analysis because of multimodal defocus curves, which would result in discontinuities of the depth of focus estimations. The following inclusion criteria were checked during an ophthalmological examination before the start of the study: visual acuity greater or equal to 0.0 logMAR, ametropia in the dominate eye lower than ± 6.0 DS and ± 2.0 DC and no known eye diseases. Participants were excluded from the study if they suffered from allergy to Cyclopentolate Hydrochloride or showed contradictions to mydriasis. Prior to the experiment, accommodation was blocked using three drops of 1 % Cyclopentolate Hydrochloride with a time duration of 30 minutes within 10 minutes in between every application. Objective refraction of the errors of the eye was achieved using a wavefront aberrometer (ZEISS i.Profiler plus, Carl Zeiss Vision GmbH, Germany) and the measurements were repeated three times to account for fluctuations of tear film and residual accommodation. The most positive reading of the objective measures were used as starting values to perform subjective distance refraction at 5 m using a single line of SLOAN letter optotypes [Bailey and Lovie-Kitchin, 2013]. The end point of the monocular refraction was the maximum plus power with the highest visual acuity. Both refraction procedures, as well as all study-related measurements, were obtained after full cycoplegic effect emerged. To control accommodation paralysis, two push-up measurements from clear to first noticeable blur in distal and proximal distance were performed. Participants with an accommodation range higher than 1 D after cycloplegia were excluded from the analysis. The study followed the tenets of the Declaration of Helsinki and was approved by the Institutional Review Board of the medical faculty of the University of Tuebingen. Informed Consent was obtained from all participants after the content and possible consequences of the study had been explained.

4.3.2 Protocol

Assessment of subjective depth of focus

Participants wore their distance correction in a trial frame (UB4, Oculus, Germany) corrected for a viewing distance of 5 m. To evaluate the subjective depth of focus, defocus curves of high contrast visual acuity in a dioptric range of ± 1.50 D within 0.5 D steps were measured. The method to calculate the depth of focus from subjective obtained defocus curve was described elsewhere [Leube et al., 2016a]. In brief, DoF is defined as the horizontal dioptric range at the threshold level of $+0.1$ logMAR below the maximum value of visual acuity. By normalizing the threshold level to

the maximum acuity value, shifts in best performance position of the defocus curve were compensated. Luminance was controlled and set to photopic light conditions of $\mathrm{L} = 250\,cd/m^2$. The assessment of the subjective depth of focus was performed under full cycoplegic conditions.

Contrast sensitivity and neural transfer function

To evaluate the contrast sensitivity [Schilling et al., 2017], a psychophysical staircase procedure (PSI Ψ method) was programmed in Matlab (Matlab 2014a, MathWorks Inc., Natick, USA) using the Palamedes Toolbox [Kingdom and Prins, 2010]. Stimuli were presented on a 120 Hz LCD display (VIEWPixx /3D, VPixx Technologies, Canada) with a 16 bit gray level resolution for each pixel. Mean luminance of the visual display was $65\,cd/m^2$ and room illumination was reduced. Prior to the measurements, the participants were light adapted for at least 10 minutes. During a four-alternative forced choice (4AFC) task, the participant was asked to respond the direction (0°, 45°, 90° or 135°) of a sinusoidal grating (Gabor Patch). The grating was enveloped with a Gaussian filter function according to Equation 8.

$$I(x,y) = I_0(\sin(2\pi f[y\sin(\theta) + x\cos(\theta)]) * e^{\frac{(x^2+y^2)}{2\sigma^2}}) \tag{8}$$

The gray scale intensity of each pixel $I(x,y)$ in the x,y position of the screen was defined by the mean gray level I_0, the frequency of a sine wave f (1/pixel) and an angular tilt θ. Stimulus size was set to 2.5° of visual angle with a Gaussian sigma of $\sigma = 0.1°$ for a viewing distance of 5 m. To achieve reliable measures for the smallest detectable contrast at each spatial frequency (from 0.5 to 60 cpd in 14 log-steps: 0.5, 1.0, 2.0, 3.0, 5.0, 7.0, 9.0, 11.0, 13.0, 15.0, 23.0, 32.0, 44.0 and 60.0 cpd), 50 trials of stimuli presentation in the adaptive staircase procedure starting with an initial Michelson contrast of 0.55 were performed. All measurements were done under cycloplegic, monocular conditions in the dominat eye while a 4 mm artificial pupil was placed in front of the participant's eye. The measured contrast sensitivity data was fitted with a double exponential function, adapted from Barten [Barten, 1999], to reduce the noise of the measurement. Individual neural transfer functions (iNTF), which require next to the CSF the optical transfer function of the eye, were implemented into image quality metrics (Equations 11-13) to calculate the objective depth of focus.

From wavefront data to the depth of focus

The method to calculate defocus curves based on wavefront measurements and derive depth of focus was described by Yi et al. [Yi et al., 2010]. Optical measurements of wavefront aberrations were performed since full cycloplegic effect emerged. Standardized Zernike coefficients from the aberrometer measurement were used to reconstruct the wavefront by summing the Zernike polynomials weighted with the coefficients. The point spread function (PSF) was calculated from the reconstructed wavefront as the Fourier transform of the pupil function. The optical transfer function (OTF) is defined by the Fourier transform of the PSF [Pedrotti et al., 2007] and refers to the direction and spatial specific properties of an optical system and also contains the modulation transfer function ($\mathrm{MTF} = \mathrm{abs}\,(\mathrm{OTF})$) as well as the phase transfer function ($\mathrm{PTF} = \mathrm{angle}\,(\mathrm{OTF})$) as a complex numbered function. A Gaussian apodization filter including a gamma of $\gamma = 0.115\,\mathrm{mm}^{-2}$ was used to model the Stiles-Crawford effect [Thibos et al., 2004].

The transfer function between object contrast and perceived contrast in the human visual systems (contrast sensitivity function, CSF) is not fully described by the optical transfer properties of the eye. A neural transfer function (NTF) describes the modulations in the perception of contrast for the retina-brain system [Campbell and Green, 1965] and has to be considered as well. The entire contrast sensitivity function can be modeled by the product of the optical and the neural transfer function [Watson and Ahumada, 2008]. Using Equation 9, the neural transfer function of the human visual system can be calculated [Michael et al., 2011].

$$NTF\,(f_x, f_y) \;=\; \frac{CSF\,(f_x, f_y)}{MTF\,(f_x, f_y)} \tag{9}$$

$$N\,(x, y) \;=\; \mathcal{F}^{-1}\,(NTF\,(f_x, f_y)) \tag{10}$$

$$VSPSF \;=\; \frac{\int_{-\infty}^{\infty} N\,(x, y) \;*\; PSF\,(x, y)\,dx\,dy}{\int_{-\infty}^{\infty} N\,(x, y) \;*\; PSF_{DL}\,(x, y)\,dx\,dy} \tag{11}$$

$$VSOTFa \;=\; \frac{\int_{-\infty}^{\infty} NTF\,(f_x, f_y) \;*\; \Re\,(OTF\,(f_x, f_y))\,df_x\,df_y}{\int_{-\infty}^{\infty} NTF\,(f_x, f_y) \;*\; OTF_{DL}\,(f_x, f_y)\,df_x\,df_y} \tag{12}$$

$$VSMTF \;=\; \frac{\int_{-\infty}^{\infty} NTF\,(f_x, f_y) \;*\; MTF\,(f_x, f_y)\,df_x\,df_y}{\int_{-\infty}^{\infty} NTF\,(f_x, f_y) \;*\; MTF_{DL}\,(f_x, f_y)\,df_x\,df_y} \tag{13}$$

In the present study, we evaluated visual Strehl metrics [Thibos et al., 2004] that are based on the optical transfer function (VSOTFa), the modulation transfer function (VSMTF) and the point spread function (VSPSF), where f_x and f_y are the spatial frequencies, x and y are the space coordinates and DL describes the diffraction limited function. For the VSOTFa, we used the augmented version proposed by Iskander [Iskander, 2006]. Visual Strehl metrics compute the optical quality normalized to diffraction limited optics and weighted by the neural transfer function (see Equations 11, 12 and 13).

Prior to the calculation of defocus curves, the measured wavefront data was scaled [Lundstrom and Unsbo, 2007] to a fixed pupil diameter of d = 4 mm and all necessary defocus steps (from - 2.0 to + 2.0 in 0.125 D steps) were converted from the refractive domain to the wavefront domain. Calculations were performed with Matlab using a reference wavelength of $\lambda = 550$ nm and a spatial resolution of 2^7 bit. Spatial frequencies ranged from 0 to 60 cycle/deg (cpd). Defocus curves and respectively the objective depth of focus were calculated for three different configurations: (1) default setting: Pupil diameter d = 4 mm, standard NTF [Campbell and Green, 1965] and setting the low order aberrations (defocus Z_2^0 and astigmatism Z_2^{-2}, Z_2^2) to zero. To account for the influence of residual lower order aberration (Parameter A), the second (2) configuration included a pupil diameter of d = 4 mm, the standard NTF [Campbell and Green, 1965] and objective Zernike terms for defocus and for primary astigmatism were corrected with the sign-switched (from error to correction) Zernike coefficients from subjective refraction. Since contrast sensitivity plays a major role for calculating visual Strehl metrics, we have incorporated in configuration (3) the individual neural transfer functions (see Equation 9) in the metric calculations (Parameter B) and re-evaluated the correlation of the subjective depth of focus and the objective defocus curves for a pupil diameter of d = 4 mm and residual lower order aberrations. The iNTF data was fitted with a double exponential square root function adopted from Barten [Barten, 1999] (see Equation 14).

To calculate the depth of focus from the defocus curves, we used threshold levels of 50 % from the maximum metric value for all three visual Strehl metrics. The workflow of the calculations is shown in Figure 9. In the standard definition of the visual Strehl metrics, the neural transfer function (NTF) from the publication of Campbell & Green is used [Campbell and Green, 1965]. In the present study, we have evaluated the NTF of the individual participants and incorporated their individual data in the calculations of the defocus curves from image quality metrics.

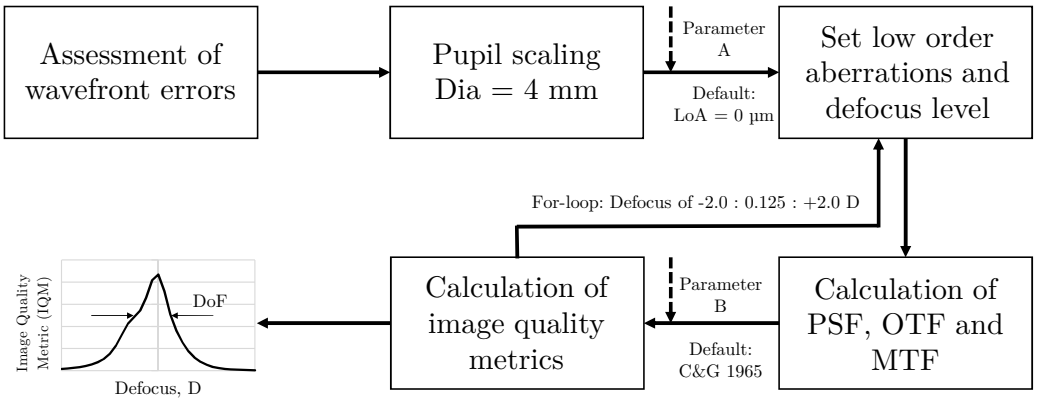

Figure 9: Workflow for calculation of through focus curve from wavefront errors using image quality metrics. The parameters A and B describe the residual low order aberrations (LoA) and the individual neural transfer function, respectively, that are evaluated regarding the DoF prediction. Dia = Pupil diameter.

4.4 Results

In total, data of 22 participants with a mean age of 26.2 ± 3.1 years and a mean spherical equivalent refractive error (M) of - 1.09 ± 2.39 D and a straight astigmatic component of $J_0 = 0.11 \pm 0.34$ D were included in the analysis.

4.4.1 Calculation of objective depth of focus from standard parameter

The mean subjective DoF evaluated from the defocus curve (mean threshold level: - 0.01 ± 0.10 logMAR) was 0.84 ± 0.27 D. Objective calculations for a pupil size of d = 4 mm gave significant lower values when the 80 % threshold was considered (DoF_{VSOTFa}: 0.37 ± 0.14 D, $p < 0.001$; DoF_{VSPSF}: 0.35 ± 0.08 D, $p < 0.001$; DoF_{VSMTF}: 0.40 ± 0.14 D, $p < 0.001$). DoF evaluated at the 50 % threshold did not result in a significant difference for all the objective metrics calculated for a 4 mm pupil size (DoF_{VSOTFa}: 0.75 ± 0.20 D, $p > 0.05$; DoF_{VSPSF}: 0.73 ± 0.23 D, $p > 0.05$; DoF_{VSMTF}: 0.86 ± 0.28 D, $p > 0.05$). By considering the default parameters and a 50 % threshold level, the computed correlations for each metric were low ($r_{VSOTFa} = 0.114$, $r_{VSPSF} = 0.174$, $r_{VSMTF} = 0.163$, $p_{all} > 0.05$) and therefore no prediction of subjective depth of focus from objective visual Strehl metrics using default settings could be achieved.

4.4.2 Parameter A - The influence of residual lower order aberrations

The correction of lower order aberrations (LoA) using trial lenses did not compensate all the errors of defocus and primary astigmatism due to the step size of 0.25 D that limits the precision of the subjective refraction. The calculation of the inaccuracy resulted

in a mean residual LoA of $0.018 \pm 0.155\,\mu$m for defocus Z_2^0 and of $0.003 \pm 0.061\,\mu$m, $-0.012 \pm 0.060\,\mu$m for oblique Z_2^{-2} and straight Z_2^2 astigmatism, respectively. Mean values of residual LoAs were nearly zero, but standard deviation showed that there was a wide range of uncorrected lower order aberrations. Figure 10 shows a comparison of defocus curves from one participant, when LoAs were set to zero (gray) and when residual LoAs were considered (black). As expected, the peak value was lower in case the residual LoAs were taken into account. Because of the asymmetry of the astigmatism, the calculations of the defocus curve can lead to asymmetric shapes that will affect the calculation of the depth of focus, see Figure 10. The mean objective DoF considering the residual astigmatism, was 0.67 ± 0.12 D for the VSOTFa, 0.74 ± 0.16 D for the VSPSF and 0.86 ± 0.20 D for the VSMTF metric. However, the recalculated defocus curves and the depth of focus for a 4 mm pupil diameter and a 50 % threshold definition showed no significant correlations between subjective and objective measures ($r_{VSOTFa} = 0.327$, $r_{VSPSF} = 0.085$, $r_{VSMTF} = 0.086$, $p_{all} > 0.05$).

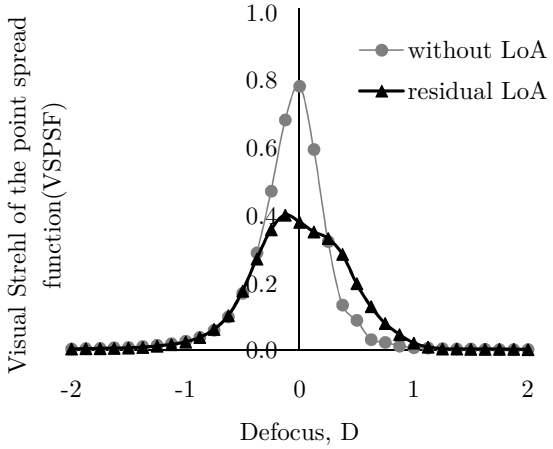

Figure 10: Comparison of defocus curves calculated without lower order aberrations (LoA) and with residual LoAs for a sample participant.

4.4.3 Parameter B The influence of the individual neural transfer function (iNTF)

The objective image quality metric VSMTF was not calculated using iNTF because the calculation of the NTF was based on the MTF that would be also used in the calculation of the VSMTF. The neural transfer function describes the fraction of the contrast sensitivity function and the modulation transfer function. To model the unknown individual neural transfer function (iNTF) for the relationship between the CSF as an output and the MTF as an optical filter of the image, we investigated respective values from both, the CSF and the MTF, for the given spatial frequencies. Figure 11a shows

that this relationship is non-linear and can be modeled by a double exponential square root function, see Equation 14 with the parameter a = 9725 and b = 25 ($R^2 = 0.95$) for an individual participant. It reflects the neural contrast gain of the visual system. Compared to the standard NTF from Campbell and Green [Campbell and Green, 1965], the mean NTF calculated from our study group (n = 22) showed a shifted maximum towards lower spatial frequencies and a lower peak value of 130.7 ± 58.8 at 6.0 cpd, Figure 11b. It is given by Equation 14 with the parameter a = 59.12 and b = 0.17.

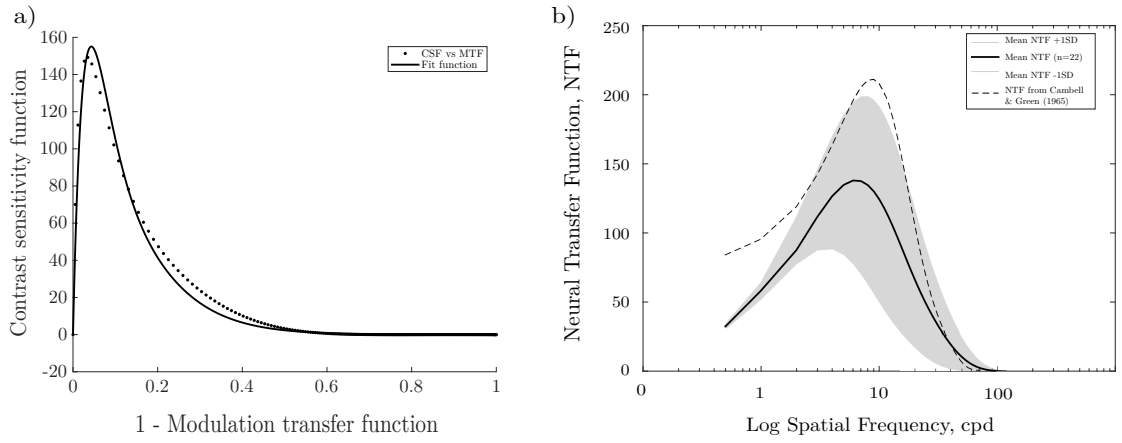

Figure 11: a) Relationship between contrast sensitivity function (CSF) and modulation transfer function (MTF). Data was fitted with a double exponential square root function (Equation 14) and represents the model of the neural transfer function (NTF). b) Comparison of mean neural transfer function from the study group (n = 22) $\pm\, SD$ and the NTF adapted from Campbell & Green [Campbell and Green, 1965]

$$NTF\,(sf) \;=\; a \,*\, sf \,*\, e^{-b*sf} \,*\, \sqrt{1 \,+\, 0.06 \,*\, e^{b*sf}} \tag{14}$$

Results of the calculations showed a wide range of individual differences in the iNTF. Objective defocus curves were calculated for VSOTFa and VSPSF, using a 4 mm pupil diameter, the individual neural transfer function and the incorporation of residual LoA. Mean objective DoF was 0.75 ± 0.15 D for the VSOTFa and 0.80 ± 0.17 D for the VSPSF metric. The correlations with the subjectively measured DoF were moderate for both metrics ($r_{VSPSF} = 0.212$, $p_{VSPSF} = 0.33$) and a statistically significant correlation was found between the objective DoF calculated using the VSOTFa and the subjective depth of focus ($DoF_{subj} \;=\; 0.74 \,*\, DoF_{VSOTFa} \,+\, 0.28$, r = 0.431, p = 0.04, Pearson) by including iNTF in the calculations of the objective DoF. However, regression analysis revealed a moderate prediction ($R^2 = 0.19$) of the subjective depth of focus. Evaluating the individual differences with and without the individual NTF provides a similar picture. The mean difference between the subjective and the objective depth of focus

using the standard NTF was 0.16 ± 0.29 D, whereas the mean difference using the iNTF was significant smaller 0.08 ± 0.28 D ($p < 0.001$, t-test).

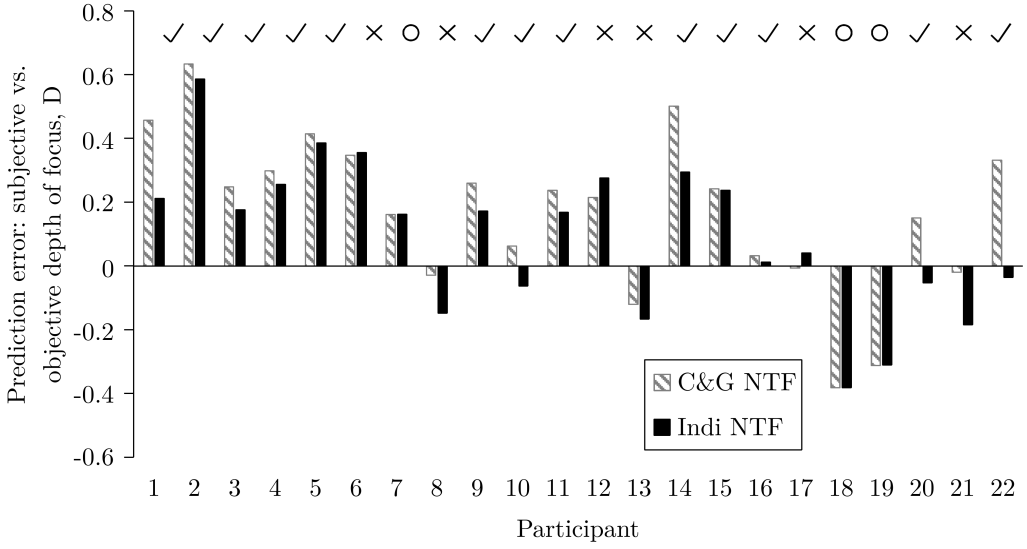

Figure 12: Individual differences between subjective and objective DoF (D) for through focus analysis using the C&G NTF [Campbell and Green, 1965] and the individual NTF. Smaller prediction errors are indicated with ✓, whereas no change is shown with ○ and higher errors are indicated by ×.

4.5 Discussion

4.5.1 Objective depth of focus and image quality metrics

The prediction of subjective depth of focus (DoF) from a single wavefront measurement has a big influence on the research in vision science. Objective assessed DoF in the current study is comparable to earlier reported values: Marcos et al. found DoF of 0.4 D for double-pass images and 1.6 times smaller values from wavefront simulations of the modulation transfer function [Marcos et al., 1999b]. They further revealed a discrepancy between the objective and subjective assessed DoF [Marcos et al., 1999b] as it ruled out in the current study using the default parameter. Yi et al. showed that the depth of focus can be calculated from through focus curves of image quality metrics for fixed thresholds [Legge et al., 1987; Marcos et al., 1999b] and estimated the objective DoF as 1.07 D for a 50 % threshold and as 0.52 D for a 80 % threshold [Yi et al., 2010]. The slightly higher values originate from the difference in pupil size, since they used a pupil diameter of 3.5 mm. They further introduced a method to calculate individual thresholds based on the root mean square of the coefficients of higher order aberrations (RMS-HOA). This method provides a higher weighting of HOA than using fixed thresholds. Nevertheless, their study gave no information about correlations

between subjective and objective depth of focus. Legras et al. investigated different definitions of objective image quality metrics (different optical parameter and spatial frequency ranges) and their impact on the prediction of subjective depth of focus, measured with adaptive optics [Benard et al., 2011; Legras et al., 2012]. The correlation coefficients were dependent on the letter size that was used for the subjective measurements. For a letter size of 0.1 logMAR (mean threshold level in the present study was - 0.01 ± 0.10 logMAR), the regression coefficients (R^2) ranged between < 0.01 and 0.1. This is in accordance with the current data, when the default settings (4 mm pupil size, LoA = 0 and NTF from Campbell & Green [Campbell and Green, 1965]) were used. The low correlation values found in the present study using the default parameters could be explained by the missing correlation between maximum visual acuity and maximum metric value ($R^2 < 0.1$, Pearson, for all three VS-metrics). Villegas et al. did not find a significant correlation between visual acuity (VA) and optical quality calculated from image quality metrics in young subjects with normal or excellent vision [Villegas et al., 2008]. It was also shown that the prediction of VA from optical quality metrics increases in low luminance condition, but is poor for bright lighting conditions [Applegate et al., 2006], which might give a hint that quality metrics are not suitable for high performance optical systems. Contrariwise, Marsack et al. found that the visual Strehl metric from the OTF can account for 81% of the average variance in high-contrast logMAR visual acuity measurements, based on three individuals [Marsack et al., 2004].

4.5.2 Pupil size dependency

There is a strong dependency of the depth of focus (DoF) on the pupil size. A smaller pupil size will produce a larger depth of focus [Marcos et al., 1999b; Ogle and Schwartz, 1959]. DoF calculated from image quality metrics does not show this dependency [Yi et al., 2010]. Furthermore, Marcos et al. showed that the objective DoF assessed by double-pass-imaging or wavefront simulations follows a non-monotonic function as the pupil size increases [Marcos et al., 1999b]. The results from the current study were evaluated for a fixed pupil diameter of 4 mm, for both, the objective and the subjective measurements. An increases in pupil size would lead to a higher optical vergence in the pupil's plane. Benard et al. found a good correlation between the induced variation of vergence within the full pupil diameter and subjectively measured depth of focus [Benard et al., 2011]. On the other hand, the Stiles-Crawford effect [Stiles and Crawford, 1933] (the luminous efficiency of the eye decrease as more off axis the light passes the pupil) limits the effect of the impact of optical vergence on the depth of focus. Furthermore, under natural viewing conditions, the subject's pupil diameter alters and is not fixed. Buehren et al. demonstrated that the correlation coefficients between

visual acuity and VSOTFa calculated from higher order aberrations becomes higher when the natural pupil diameter is considered ($r = 0.56$, $p < 0.1$) while correlations using a fixed 3 mm pupil diameter were worse ($r = 0.43$, $p > 0.1$) [Buehren and Collins, 2006].

4.5.3 Monochromatic and polychromatic aberrations

Calculations of residual lower order aberrations and their incorporation into the evaluation of the depth of focus from objective defocus curves resulted in asymmetric shapes (Figure 10). One can expect that this asymmetry causes an increase of the individual variations of the depth of focus, when the DoF is predicted from image quality metrics using objective defocus curves. But these correlation coefficients did not changed by taking residual LoAs into account, an observation that was supported by Yi et al. [Yi et al., 2010]. The authors reported that the correlation of the estimated VSOTF threshold and the RMS-HOA dropped down, when the residual astigmatism was considered. Results from Thibos et al. showed that a subjective refraction via optimized visual acuity is not based on the criterion of minimizing the wavefront variance [Tarrant et al., 2010] like it is done by setting the lower order aberrations to zero [Thibos et al., 2002b]. The used method from the current study to estimate residual lower order aberration by correcting the Zernike terms by the sign-switch coefficients from the subjective refraction could be disadvantageous. The usage of adaptive optics systems [Marcos et al., 2017] to correct lower and higher order aberrations would be preferred in future studies to investigate the neural involvement [Yoon, 2010] and the effect of lower order aberrations on the depth of focus.

All calculations of optical quality parameters were performed for monochromatic light and a reference wavelength of $\lambda = 550$ nm, according to the eye's photopic spectral sensitivity. Because aberrations are a function of the wavelength (see also the section "From wavefront data to the depth of focus" in the methods), the presented results will be different if the reference wavelength is changed. Subjective measures were performed in polychromatic white light conditions. Recalculation of metric values using polychromatic point spread function [Ravikumar et al., 2008] will lead to different through focus curves from objective image quality metrics and to a change in correlations between objective and subjective depth of focus. Nevertheless, the range of the focal shift associated with the longitudinal chromatic aberration [Thibos et al., 1992] weighed by photopic spectral sensitivity of the eye would result in a difference of 0.3 D and since it is a general model, the polychromatic calculation would not result in an enhancement of the individual prediction performance.

4.5.4 Individual neural transfer function iNTF

Calculating the neural transfer function (NTF) as the fraction between the contrast sensitivity function (CSF) and the modulation transfer function (MTF) was shown to provide good predictability regarding the visual acuity [Watson and Ahumada, 2008] and can serve as good approximation for the NTF. However, a more precise and straightforward assessment of the NTF would be to use interference fringes [Campbell and Green, 1965; Ahumada and Coletta, 2009]. The comparison of the NTF measured with interference fringes by Campbell & Green [Campbell and Green, 1965] and the calculated NTF from current study showed that the calculations result in lower NTF's. This is explained by the fact that using interference fringes by passes the eye's optic dynamically and is furthermore a diffraction limited measurement. The incorporation of individual calculated NTF into the VSOTFa metric leads to an increase of the correlation coefficient to $r = 0.43$, with the result that the subjective depth of focus can be predicted from the objective measures. The increase in individual information which is provided for metric calculations by the additional individual NTFs produce an expectable enhancement of the goodness of the correlation. Individual neural transfer function gives similar measures of contrast transfer as the OTF, since both characterize the modulation of contrast for different spatial information of an optical system. On the contrary, visual acuity estimates a threshold level of the smallest resolvable spatial detail and is defined as the cutoff frequency. This fundamental difference in measures leads to challenging problems while comparing the area under the optical transfer functions and a single acuity value. For the depth of focus, the estimation and judgment of blur, the contrast of the perceived image seems to play a major role.

The present study investigated how the correlation between objective DoF estimations from image quality metrics can provide moderate predictions for subjective DoF. Calculations from the VSOTFa metric resulted in superior correlation when compared to the VSPSF and VSMTF metric. However, the parameter residual lower order aberrations do not explain the major variance of subjective measures. For the prediction of subjective DoF using the VSOTFa metric, the CSF of the individual eye plays a major role and its incorporation using the iNTF into the visual Strehl metrics results in a moderate, significant correlation between the objective and the subjective DoF. The results of the study could enable scientists as well as industry in ophthalmology and vision science to develop individualized solutions for a better performance of intraocular lenses or vision after refractive surgery in the future. This will improve current methods that only take standardized measures into account.

Acknowledgements

This work was done in an industry-on-campus-cooperation between the University Tuebingen and Carl Zeiss Vision International GmbH. The work was supported by third-party-funding (ZUK 63). We would like to thank Larry Thibos and Matt Jaskulski for providing us with the calculation routine of polychromatic point spread functions and the anonymous reviewer for their concise reviews.

Author contributions statement

All authors were involved in the design, the reasoning, interpretation, and summarizing of the study and the key contributions were as follows: A. L., T. S., D. K., G. A. O., M. D. F. and A. O. developed the study protocol and did the data recording and S. W. was the principal investigator. All authors reviewed the manuscript.

Additional information

A. Ohlendorf and S. Wahl are employees of Carl Zeiss Vision International GmbH.

5 Sign-dependent response to spherical defocus under monochromatic light conditions

Leube, A., Kostial, S., Alex Ochakovski, G., Ohlendorf, A., & Wahl, S. (2018). Symmetric visual response to positive and negative induced spherical defocus under monochromatic light conditions. Vision Research, 143, 52-57. doi:10.1016/j.visres.2017.12.003

5.1 Abstract

The purpose of the study was to investigate the sign-dependent response to real and simulated spherical defocus on the visual acuity under monochromatic light conditions. The investigation included 15 myopic participants with a mean spherical equivalent error of - 2.98 ± 2.17 D. Visual acuity (VA) was tested with and without spherical defocus using the source method (simulated defocus) and the observer method (lens-induced defocus) in a range of ± 3.0 D in 1.0 D steps. VA was assessed using Landolt C's, while the threshold was determined with an adaptive staircase procedure. Monochromatic light conditions were achieved using band pass filters with a wavelength of 450 ± 2 nm, 530 ± 2 nm and 630 ± 2 nm. Results showed that the reduction of VA was significantly different under blue lighting conditions, when compared to the green and red light conditions. No significant difference in the reduction of the VA was found between the positive and the negative sign of defocus for all lighting conditions. The agreement for the VA between the source and observer method was significantly dependent on the wavelength as well as on the level of defocus. To conclude, under monochromatic light conditions, myopes show a symmetric sign-dependency regarding the influence of spherical defocus on visual acuity. The observed results indicate that the human visual system is capable of integrating the chromatic differences in refraction to distinguish between the signs of defocus.

5.2 Introduction

The assessment of subjective visual performance, e.g. visual acuity or contrast sensitivity, in the presence of optically induced aberrations is a widely studied measure and applied in every assessment of the subjective refractive error [Benjamin, 2006]. It could be used for example, to judge the goodness of an optical correction [Kasper et al., 2006; Hayashi et al., 2000; Lundstrom et al., 2007], to gain deeper insights in the understanding of the visual system [Artal et al., 2004; Atchison et al., 2009b; Atchison and Mathur, 2011; Ohlendorf et al., 2011] or to investigate how combinations of optical aberrations can be used to enhance visual perception [Applegate et al., 2003; de Gra-

cia et al., 2010; Mon-Williams et al., 1998]. In particular, spherical defocus results in a rotational-symmetric blur circle in the retina plane and leads to a deterioration of the visual performance [Bradley et al., 1991; Charman, 1979; Jansonius and Kooijman, 1998; Sehlapelo and Oduntan, 2007]. Although a change in the sign of the induced defocus would result physically in the same size of the blur circle, psychophysical measurements under polychromatic light conditions of human visual perception revealed an asymmetric reduction of visual acuity [Radhakrishnan et al., 2004b; Leube et al., 2016b] and contrast sensitivity [Radhakrishnan et al., 2004a], depending on the sign of the optically imposed defocus.One explanation for the observed differences could be the interaction of the induced spherical defocus with inherent higher order aberrations, where the distribution of light at the paraxial plane is not symmetric anymore and acts as a directional cue for the visual system [Guirao and Williams, 2003]. On the other hand, the chromaticity of visual stimuli together with the chromatic aberration of the human eye [Marcos et al., 1999a; Thibos et al., 1992; Le Grand, 1964; Thibos et al., 1990] was also discussed as a factor that allows the visual system to identify the sign of defocus [Ohlendorf and Schaeffel, 2009] and it was shown that this cue provides directional information for the accommodative system [Kruger et al., 1995; Kruger and Pola, 1986; Lee et al., 1999].

Therefore, the first hypothesis of the current study was that under monochromatic light conditions, the sign of an induced spherical defocus has no influence on the reduction of the visual acuity. Next to induce blur by the use of defocusing lenses (called observer method [Chan et al., 1985]), it is possible to deteriorate the displayed image itself by using Fourier optics and this is referred to the source method [Chan et al., 1985]. Simulations of blur and the comparison to lens induced blur were shown to result in good agreement investigating astigmatism ($\Delta\text{VA} = 0.17 \pm 0.05\,\text{logMAR}$) [Ohlendorf et al., 2011] and positive spherical defocus ($\Delta\text{VA} = 0.14 \pm 0.04\,\text{logMAR}$) [Dehnert et al., 2011].

The major difference between the observer and the source method is that the simulation (in case of the source method) results in a blurry image without inducing optical vergence at the same time. From accommodation theory it is known that blur perception is also driven by induced optical vergence [Fincham, 1951] and not blur alone [Kruger and Pola, 1986; Del Aguila-Carrasco et al., 2017; Esteve-Taboada et al., 2017]. Therefore, the second hypothesis was that a symmetric reduction of visual acuity occurs, when tested under a blur-only condition (source method).

In brief, the purpose of the current study was to investigate the sign-dependent subjective sensitivity to spherical blur in (1) monochromatic light conditions and (2) under blur-and-vergence and blur-only conditions.

5.3 Methods

To assess the visual performance under monochromatic light conditions, high contrast visual acuity was measured in two experimental blur conditions: 1) lens induced blur (observer method) and 2) simulated blur (source method) [Chan et al., 1985]. Both blur conditions were designed with the same psychophysical setup and followed the same staircase procedure to measure the visual acuity.

5.3.1 Participants

A prospective, randomized study was carried out at the University Tuebingen enrolling 15 healthy participants (9 male and 6 female) with a mean age of 27.2 ± 3.4 years and a mean spherical equivalent refractive error of -2.98 $\pm$ 2.17 D (range from 0.25 D to - 6.00 D). Inclusion criteria for participation were a refractive error of less than 0.25 D (range - 0.25 D to - 6.0 D), less than - 2.00 D of astigmatism and best corrected visual acuity of 0.1 logMAR (6/7.5) or better. Participants with pre-existing ocular diseases were not allowed to take part in the study. All subjects were naïve to the purpose of the experiment. The study course was approved by the Ethics Commission of the Medical Faculty of the University of Tuebingen. The research followed the tenets of the Declaration of Helsinki. Informed consent was obtained from all subjects after explaining the nature and possible consequences of the participation in the study.

5.3.2 Protocol

All participants were screened for ocular health by an ophthalmologist. Thereafter, particiaptan's pupils were dilated and physiologic accommodation was inhibited by the administration of a total of 3 drops of a cycloplegic agent (1% Cyclopentolate Hydrochloride; Alcon Ophthalmika GmbH, Austria) in participant's dominant eye, 1 drop at a time in 10 minute intervals. Prior to the study, the objective refraction and the pupil size were measured with an aberrometer (ZEISS i.Profiler plus, Carl Zeiss Vision GmbH, Aalen, Germany). The subjective refractive error was assessed using a trial frame (UB4, Oculus, Germany) and trial lenses with an artificial pupil of 4 mm diameter under photopic conditions ($L = 250\, cd/m^2$). To control the emerged effect of the cycloplegic agent, push-up measurement [Chen and O'Leary, 1998] was performed before, in between and after the study measurements. Participant's were given a training session prior to the visual acuity tests in order to familiarize them with the keypad

and the staircase procedure. After the training, visual acuity was assessed under monochromatic conditions, using bandpass filters with central transmission wavelengths of 450 ± 2 nm (blue), 530 ± 2 nm (green) and 630 ± 2 nm (red) and a full half width maximum of 10 nm (Newport Corporation). Luminance was set to 1 cd/m^2 in both methods (lens induced defocus or simulated defocus). To obtain the same luminous conditions for each filter, the luminance settings of the monitor were adjusted according to the specified transmission profile. Furthermore, spherical refractive errors were corrected for each filter separately, in order to account for changes in refraction due to chromatic aberration. The measurement sequences of the defocus level, the filter condition and the method (observer vs. source method) were completely randomized. All psychophysical measurements were performed with correction of refractive errors using a trial frame, on a distance between eye and display of 5.0 m and for a back-vertex-distance between trial frame and eye of 12 mm. The contrast of the stimulus was above 0.98.

To investigate the effect of the sign of defocus, the induced spherical defocus ranged from + 3.0 D to - 3.0 D in 1.0 D steps. In case the observer method was applied, the induced blur was produced by trial lenses placed in a trial frame and using an artificial pupil of 4 mm diameter. To simulate the blur in the displayed image (source method), a Fourier optics approach similar to the algorithm from Legras et al. was used and participants pupil size was controlled by using a 4 mm artificial pupil [Legras et al., 2004]. The image of the Landolt C was converted to the frequency domain using Fourier transformation and multiplied by the calculated optical transfer function [Thibos et al., 2002a] of the defocus in regards to the given wavelength and pupil diameter. Visual acuity was tested for both blur conditions and each defocus level according to a BestPEST [Kingdom and Prins, 2010; Bach, 1996] adaptive staircase procedure incorporating 24 trials per threshold estimation, a fixed slope of the psychometric function of 2.0 and high-contrast Landolt C's as standard optotypes in eight possible directions (guessing rate of 0.125). The displayed image size was corrected for spectacle magnification using a distance between the lens and the principal plane of the eye of h = 15 mm [Benjamin, 2006; Chan et al., 1985]. The visual acuity test was programmed in MATLAB (2016a, The MathWorks, Inc., Natick, USA) using the Palamedes toolbox [Kingdom and Prins, 2010] (Version: 1.8.2, 2016) and the Psychtoolbox [Kleiner et al., 2007] (Version: 3.0.13).

5.3.3 Analysis

To compare the reduction of visual acuity under different conditions, the slope of the regression line for visual acuity over defocus was analyzed. For the statistical analysis, repeated measurements analysis of variance was applied (IBM SPSS Statistics, IBM Corp., Armonk, NY), including the factors filter condition (blue, green and red), method (source and observer) and the sign of the induced defocus (positive and negative). Level of significance was set to $\alpha = 0.05$.

5.4 Results

5.4.1 Chromatic change of refraction and residual accommodation

The spherical refractive error of the participant's eye was adjusted for each filter condition separately to ensure that the best focus position was similar for the three tested wavelengths. The refractive error was shifted by - 1.07 ± 0.27 D for the 450 nm filter, - 0.25 ± 0.16 D for the 530 nm and $+ 0.22 \pm 0.21$ D in the 630 nm light condition. The average residual accommodation after cycloplegia was 0.48 ± 0.08 D and there was no significant change during the time course of the experiment ($p > 0.05$, t-test).

5.4.2 Reduction of visual acuity with spherical defocus

Comparing the non-defocused visual acuity under monochromatic conditions, visual acuity was significantly lower under the blue light condition ($VA_{450} = 0.22 \pm 0.16$ logMAR, $p < 0.001$, ANOVA, Bonferroni corrected) but not different ($p = 0.49$, ANVOA, Bonferroni corrected) for the green light condition ($VA_{530} = 0.00 \pm 0.13$ logMAR) and the red light condition ($VA_{630} = - 0.09 \pm 0.13$ logMAR). A linear relationship between the logarithmic visual acuity and the induced spherical defocus was observed for real blur ($R^2 \geq 0.95$) and simulated blur ($R^2 \geq 0.97$), see Figure 13. In both blur conditions (the source and the observer method), the within-subjects difference in the reduction

Table 1: Mean ± SD slope of reduction of visual acuity (logMAR/D) for the source and the observer method and all three monochromatic light conditions

Sign of defocus		Slope of reduction of visual acuity, logMAR/D		
		450 nm	530 nm	630 nm
Source method	positive	0.22 ± 0.05	0.26 ± 0.04	0.25 ± 0.04
	negative	0.23 ± 0.03	0.26 ± 0.04	0.25 ± 0.04
Observer method	positive	0.25 ± 0.04	0.29 ± 0.05	0.32 ± 0.04
	negative	0.25 ± 0.05	0.30 ± 0.04	0.32 ± 0.05

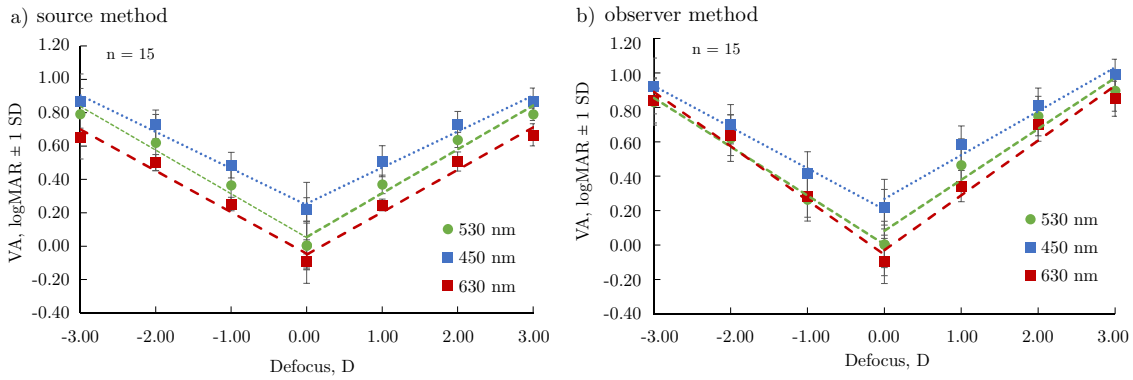

Figure 13: Reduction of visual acuity due to spherical defocus in monochromatic light conditions

of visual acuity due to the induced spherical defocus was independent from the sign of defocus in all light conditions (observer method: $F(2,28) = 0{,}301$, $p = 0.742$; source method: $F(2,28) = 1.284$, $p = 0.292$). But when compared to blue light conditions, the reduction was steeper in red and green light condition for the observer method (see Table 1).

5.4.3 Comparison between real and simulated blur (observer vs. source method)

The reduction of visual acuity (the slope of linear regression) was significantly different between the methods in each filter condition ($F(2,28) = 11.720$, $p < 0.001$). Figure 14 shows the agreement for the mean visual acuity between the observer method and the source method for all used defocus steps and the blue (a), green (b) and red (c) light conditions. The values for the analysis of the absolute differences, as reported in Table 2, reveal an increase of difference between the two methods with higher levels of defocus for the red wavelength condition (positive induced defocus: $r = 0.93$, $p = 0.07$; negative induced defocus: $r = 0.98$, $p = 0.02$, Pearson), but not for the green and blue wavelengths. Furthermore, the blur simulation of the source method tends to underestimate the visual acuity, when negative spherical defocus is induced.

Table 2: Mean absolute difference between the real and simulated blur condition SEM for all defocus levels (D) and wavelengths (nm)

λ, nm	Defocus level, D					
	-3.0	-2.0	-1.0	+1.0	+2.0	+3.0
450	0.08 ± 0.02	0.10 ± 0.04	0.13 ± 0.02	0.11 ± 0.00	0.10 ± 0.02	0.10 ± 0.02
530	0.08 ± 0.02	0.11 ± 0.03	0.16 ± 0.02	0.16 ± 0.02	0.10 ± 0.02	0.12 ± 0.07
630	0.17 ± 0.03	0.15 ± 0.02	0.09 ± 0.03	0.10 ± 0.02	0.20 ± 0.02	0.19 ± 0.03

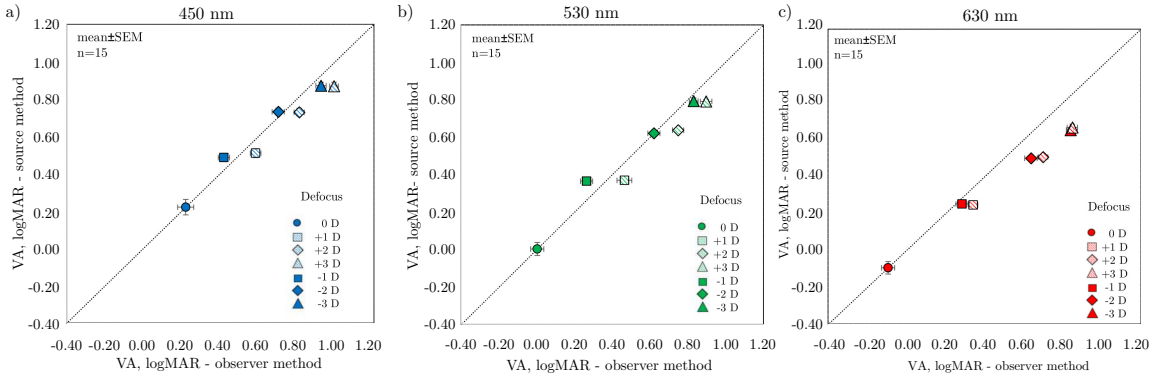

Figure 14: Comparison of mean visual acuity SEM obtained with source (ordinate) and observer (abscissa) method in blue (a), green (b) and red (c) light conditions. The dashed bisecting reference line corresponds to perfect agreement.

5.5 Discussion

The asymmetrical response of myopes to negative or positive induced spherical defocus on visual acuity and contrast sensitivity was reported previously [Radhakrishnan et al., 2004b; Leube et al., 2016b; Radhakrishnan et al., 2004a], but the stimuli that were used in these studies were polychromatic. Chromatic aberration of the eye causes a shift of the best corrected refractive error for shorter wavelengths, compared to longer wavelengths of around 1.30 D between 450 nm and 630 nm, this result is comparable to previously published data [Marcos et al., 1999b; Thibos et al., 1992]. This information could be used by the visual system as a directional cue for the identification of the sign of defocus, in case polychromatic stimuli are used [Ohlendorf and Schaeffel, 2009]. The results of the current study showed no asymmetry in the reduction of visual acuity between positive and negative induced spherical defocus in monochromatic light conditions, it is possible that the identification of the sign of the defocus by the visual system fails under these conditions. Furthermore, even if the effect of the induced optical vergence is suppressed by the use of the source method, the reduction in visual

acuity is perfectly symmetric for monochromatic stimuli between positive and negative defocus. No influence on the effect of monochromatic blur on visual acuity could be found in the presences or absence of light vergence. Therefore, the results of the current study suggest that previously reported asymmetry in visual response [Radhakrishnan et al., 2004b; Leube et al., 2016b; Radhakrishnan et al., 2004a] originates from an functional integration over monochromatic light channels and that the chromaticity act as directional cues to determine the sign of defocus. Since the visual acuity seems to be unaffected by the absence of the light vergence it is suggested that the high spatial frequency channels have no input from light vergence for the detection of the sign of defocus, or in any case, its input does not affect VA. Further investigations will have to show if the results are valid also for low-frequency channels in the visual system, as it is known that accommodation responds best to light vergence at intermediate spatial frequencies of around 3 - 5 cycles per degree [Mathews and Kruger, 1994].

The question raises whether this discrimination of the defocus sign takes place already at the retinal level or whether higher cortical levels of the visual system sensitive to the sign of defocus. Previous studies have shown that the asymmetry between positive and negative induced defocus occurs monocularly and therefore have to be determined on the retinal level [Ohlendorf and Schaeffel, 2009]. By adjusting the image size during the visual acuity measurements, we ensured a constant retinal image throughout all defocus levels. Therefore we can exclude differences in visual processing throughout changing of receptive field sizes and assume a retinal mechanism of detection. However, in chicken it was shown that the detection of the sign of defocus is not based on the retinal image size estimations [Curry et al., 1999; Schmid et al., 1999].

5.5.1 Depth of focus, luminance and higher order aberrations

With the use of a cycloplegic agent, we could exclude accommodation as a confounding factor that could influence our results. However, the measured residual accommodation, assessed by the push-up method [Chen and O'Leary, 1998], represents the combined effect of residual accommodation and the natural depth of focus of the eye that can range between 0.4 D and 2.0 D for a 4 mm pupil size [Leube et al., 2016a]. Compared to Radhakrishnan et al., the observed residual accommodation in our study was higher, probably because the size of the artificial pupil was smaller and therefore the depth of focus was larger [Radhakrishnan et al., 2004b]. To further account for the influence of the depth of focus, future studies will need to assess the sign-dependent response under monochromatic light conditions in different pupil sizes.

In addition, using smaller increments of induced defocus, especially between induced defocus of 0 D and 2 D should be investigated. The step size of 1 D, used in this study, was chosen due to the high number of investigated parameters in order to reduce measurement time.

The design of the current study involved the same luminance settings for all three wavelength conditions. The definition of luminance including the luminous flux that give a measure of physical electromagnetic radiation weighted by the luminosity function of the eye [Wyszecki and Stiles, 2000] and the narrow bandwidth of FHWM = 10 nm of the used filter limited the light level to $1\,\mathrm{cd/m^2}$. Since the luminance was constant throughout the different wavelength conditions, any effect of the luminance on the observed results can be ruled out. Johnson et al. revealed a linear relationship between background luminance and visual acuity [Johnson and Casson, 1995] and it can be assumed that the reported results are also valid for photopic light levels.

Lower order aberration, like spherical defocus and astigmatism, were corrected using trial lenses. Nevertheless, the eye's optic might additionally be affected by higher order aberrations like coma or spherical aberration [Villegas et al., 2008; He et al., 2000; Hartwig and Atchison, 2012]. Jansonius and Kooijman showed that the interaction between a higher amount of spherical aberration and the induced spherical defocus could lead to a shift in optimum focus [Jansonius and Kooijman, 1998] and Radhakrishnan et al. concluded that this explains the phenomena of asymmetry in visual acuity of positive and negative induced defocus [Radhakrishnan et al., 2004b]. In our study cohort, the root-mean-square (RMS) value of higher order aberration ($\mathrm{RMS}_{HOA} = 0.08 \pm 0.03\,\mu\mathrm{m}$) was small compared to other studies [Hashemi et al., 2015; Francisco Castejon-Mochon et al., 2002] and therefore highly unlikely to have influenced the results. However, a mutual interaction would have affected both of the used blur conditions in the same manner and the blur-only condition (source method) showed a symmetric reduction of the visual acuity. Therefore, any interaction of HOA with the induced defocus can be omitted.

Simulating optical blur and degrade images by using a Fourier approach was shown to agree with lens induced blur since positive lenses are used [Ohlendorf et al., 2011; Dehnert et al., 2011]. Legras et al. developed a numerical model that incorporates the inverse individual higher order aberrations of the eye to simulate the impact of the spherical defocus alone [Legras et al., 2004]. In the current study design, image simulations were performed in the frequency domain by Fourier transform for pure defocus effects. Because the observer method (blur + optical vergence) involved interaction

between inherent higher order aberrations and the induced defocus, the displayed image from the source method (blur alone) was calculated from spherical alone. The retinal image would be the result from the displayed image further degraded by the higher order aberrations of individual's eye in the same manner as it is true for the observer method.

The chromatic dispersion of the refractive media in the eye leads, next to an axial shift in refraction, additionally to differences in chromatic magnification for extended objects. In a first approximation, this difference in magnification ΔMag is proportional to the difference in refraction ΔR_x [Thibos et al., 1991] and lead to differences in retinal stimulus size. However, the individual chromatic magnification factors in the current study were small ($< 2.0\%$) and do not explain the lower values for the blue light condition. Pokorny et al. found worse grating acuity in blue light compared to green and red gratings [Pokorny et al., 1968] and addressed this difference to physiological factors, like the blue and green mechanism [Stiles, 1946] and the higher neural convergence in blue receptors [Brindley, 1954]. However, other studies [Hartridge, 1946; Roaf, 1930] could not found difference in monochromatic blue light conditions but used broadband filters to restrict the light spectrum.

5.5.2 Implications for the emmetropization of the eye

The reported finding have possible implications for the understanding of the emmetropization of the eye. Wildsoet et al. concluded from chicken experiments that the chromatic aberration is not fundamental for the emmetropization process of the chicken eye, but may be essential for fine tuning the refraction [Wildsoet et al., 1993]. Later, Seidemann and Schaeffel reported on shifts in accommodation tonus in humans and chicken since quasi-monochromatic illumination conditions are used and they concluded that several cone types contribute to the process of emmetropization [Seidemann and Schaeffel, 2002]. Our findings support these conclusions by showing that the identification of the sign of defocus is triggered by the chromaticity of the light and the chromatic aberration of the eye.

5.6 Conclusion

Symmetric response of visual acuity to positive and negative induced spherical defocus was observed under monochromatic lighting conditions. Chromatic aberration of the eye show asymmetric shift of refraction in best corrected vision for short-, medium- and long wavelength monochromatic light. Since previous studies have found an asymmetry under polychromatic conditions in a visual acuity task, we conclude that the visual system uses the chromaticity of light and the chromatic aberration of the eyes optics to identify the sign of defocus, but not the presence of light vergence. The current findings may additionally give some further insights into the emmetropization of the eye and the development of myopia.

Acknowledgements

This work was done in an industry-on-campus-cooperation between the University Tuebingen and Carl Zeiss Vision International GmbH. The work was supported by third-party-funding (ZUK 63). A. Leube, S. Kostial, A. Ochakovski, A. Ohlendorf and S. Wahl report no financial interests or potential conflicts of interest.

Disclosure

This study was conducted by the Institute for Ophthalmic Research, University of Tuebingen. A. Ohlendorf and S. Wahl are employees of Carl Zeiss Vision International GmbH. All authors were involved in the design, the reasoning, interpretation, and summarizing of the study and the key contributions were as follows: A. Leube, S. Kostial, A. Ochakovski and A. Ohlendorf developed the study protocol and did the data recording and S. Wahl was the principal investigator.

6 Summary

The main purpose of the presented work was to study the subjective and objective tolerance of the visual system to different optical aberrations. Investigations covered the influence of lower order astigmatism on the subjective depth of focus (sDoF), the effect of the individual neural transfer function on the prediction of sDoF from objective through focus curves calculated from image quality metrics. Finally, the examination of possible causes for differences between positive and negative imposed spherical defocus on the visual acuity were investigated. In summary, the presented results lead to the following conclusions:

(1) Small amounts of induced primary astigmatism enhance the sDoF without a major degradation of visual performance. However, the capability to enhance subjective depth of focus is higher if the astigmatism is induced in 90° direction (with-the-rule astigmatism). Since lower order aberrations like astigmatism can be incorporated into spectacle lenses, the investigated approach is capable to be used for novel optical designs in PAL's or IOL's.

(2) The assessment of sDoF using psychophysical methods is an exhausting procedure, especially if different optical corrections should be compared. The use of trough focus curves, estimated from visual Strehl metrics, was shown to provide objective measures for the depth of focus, but correlations to the subjective depth of focus are low. The developed methods link subjective assessed contrast vision to objectively obtained wavefront errors and enable the calculation of individual image quality metrics. The incorporation of the individual neural transfer function based on the eye's contrast sensitivity function (CSF) improves the predictability of sDoF. In combination with fast assessment methods for the CSF, the given results can be transferred to the clinical pre-assessment of best individual optical correction for presbyopia.

(3) Methodological use of through focus curves in the presented work showed that induced positive spherical defocus results in a stronger reduction in visual performance (high contrast visual acuity) as compared to the same amount of negative defocus. Measurement protocol required the use of polychromatic light conditions. Further investigations which controlled the light's spectrum towards narrow monochromatic conditions revealed a symmetric response of visual performance. These results give evidence that the human visual system integrates the asymmetry in chromatic aberration of the eye's optical media to be able to detect the sign of defocus. This could lead to further developments in presbyopia corrections that

use a specific design of chromatic aberration to beneficially influence the depth of focus based on wavelength-dependent shifts in sensitivity.

Future work, based on the results of the present work, should investigate the clinical feasibility of presbyopia corrections using the approach of induced astigmatism. Furthermore, the difference between an induced with-the-rule and an induced against-the-rule astigmatism in their capability to enhance the depth of focus has to be investigated. Simulated retinal image analysis could be used to estimate possible interactions with the induced astigmatism, inherent higher order aberrations and the orientation of visual stimuli. In addition to conventional simulations of retinal images, calculations for polychromatic transfer functions can be performed. It should be analyzed whether polychromatic estimations of objective depth of focus could explain the missing variance in the prediction of the subjective depth of focus. Since measurements under monochromatic light conditions revealed symmetric response between positive and negative induced spherical defocus, further experiments are needed to clarify whether contrast adaption takes place under these conditions. Additionally, the role of contrast adaptation in monochromatic light during the emmetropization of the eye should be investigated.

7 Zusammenfassung

Das Ziel der Arbeit war die Untersuchung der subjektiven und objektiven Sensitivität des visuellen Systems gegenüber verschiedenen optischen Aberrationen. Die Untersuchungen umfassten zum einen Messungen hinsichtlich der Auswirkungen des primären Astigmatismus auf die subjektive Schärfentiefe (sDoF). Zum anderen wurde die Bedeutung der individuellen neuronalen Übertragungsfunktion für die Vorhersagbarkeit der sDoF aus objektiven Defokuskurven, die aus Bildqualitätsmetriken berechnet wurden, behandelt. Des Weiteren wurden Untersuchungen zu möglichen Ursachen des Unterschiedes zwischen positivem und negativem sphärischem Defokus bezüglich der Reduktion der Sehschärfe durchgeführt. Zusammenfassend lassen sich aus den dargestellten Ergebnissen folgende drei Schlussfolgerungen ableiten:

(1) Geringe Beträge eines induzierten primären Astigmatismus erhöhen die sDoF, ohne dass die Sehleistung signifikant beeinträchtigt wird. Die Möglichkeit, die subjektive Schärfentiefe zu erhöhen, ist jedoch erfolgversprechender, wenn der Astigmatismus in 90° Richtung induziert wird (Mit-der-Regel Astigmatismus). Da Aberrationen niedrigerer Ordnung, wie der primäre Astigmatismus auch in Brillengläsern induziert werden können, ist es mit Hilfe dieser Erkenntnisse möglich, neuartige optische Designs in Gleitsichtgläsern oder Intraokularlinsen zu entwickeln.

(2) Die Beurteilung der sDoF mittels psychometrischer Methoden ist ein langwieriges Verfahren, insbesondere wenn verschiedene optische Korrekturen verglichen werden sollen. Es konnte gezeigt werden, dass die Verwendung von objektiven Defokuskurven Messwerte für die Schärfentiefe liefern, allerdings sind die Korrelationen zur subjektiven Schärfentiefe gering. Die in dieser Arbeit beschriebenen Methoden verknüpfen subjektiv ermittelte Kontrastsensitivität mit objektiven Wellenfrontfehlern und ermöglichen die Berechnung individueller Bildqualitätsmetriken. Die Einbeziehung der individuellen neuronalen Transferfunktion auf Basis der Kontrastempfindlichkeitsfunktion (CSF) des Auges verbessert die Vorhersagbarkeit der individuellen sDoF aus objektiven Messungen. In Kombination mit effizienteren Messmethoden der CSF können die Ergebnisse in die klinische Anwendung übertragen und zur Entwicklung verbesserter, individueller optischer Korrekturen der Alterssichtigkeit genutzt werden.

(3) Die Ermittlung von Defokuskurven in der vorliegenden Arbeit zeigte, dass induzierte positive sphärische Defokussierung bei Stimuli mit hohem Kontrast im Vergleich zu gleich großer negativer Defokussierung zu einer stärkeren Reduktion der Sehleistung führt. Dieser Effekt tritt auf, sofern polychromatische Lichtverhältnisse zur Verwendung kommen. Weitere Untersuchungen unter schmalbandigen, monochro-

matischen Verhältnissen, ergaben eine symmetrische Reduktion der Sehleistung. Diese Ergebnisse zeigen, dass das menschliche Sehsystem auch die Asymmetrie der chromatischen Aberration der optischen Medien des Auges nutzt, um das Vorzeichen der Defokussierung zu detektieren. Dies könnte zu weiteren Entwicklungen von Korrektionsmitteln für die Altersichtigkeit führen, die mit Hilfe einer spezifischen chromatischen Aberration die Schärfentiefe durch wellenlängenabhängige Empfindlichkeitsverschiebungen positiv beeinflussen könnten.

Weiterführende, auf den Ergebnissen der vorliegenden Arbeit basierende Untersuchungen, sind notwendig um die klinische Umsetzung von neuartigen Presbyopiekorrektionen mit dem Ansatz des induzierten Astigmatismus zu verifizieren. Darüber hinaus sollte die Ursache des Unterschiedes zwischen einem induzierten Astigmatismus mit der Regel und einem induzierten Astigmatismus gegen die Regel in Bezug auf ihre Auswirkung auf die Vergrößerung der Schärfentiefe weiter untersucht werden. Mit Hilfe optisch, simulierter Netzhautbilder können mögliche Wechselwirkungen eines induzierten Astigmatismus, inhärenten Aberrationen höherer Ordnung und der Orientierung visueller Reize abgeschätzt und analysiert werden. Neben konventionellen Simulationen von Netzhautbildern können auch Berechnungen für polychromatische Übertragungsfunktionen durchgeführt werden. Es sollte untersucht werden, ob polychromatische Berechnungen der objektiven Schärfentiefe die fehlende Varianz in der Vorhersage der subjektiven Schärfentiefe erklären könnten. Da die Messungen unter monochromatischen Lichtverhältnissen eine symmetrische Reaktion auf positivem und negativem induziertem sphärischem Defokus zeigten, müssen weitere Experimente klären, ob unter diesen Bedingungen eine perzeptuelle Kontrastaadaptation stattfindet und welches Rolle diese bei der Emmetropisierung des Auges spielt.

8 References

Ahumada, A. J. and Coletta, N. J. (2009). Neural transfer functions from interferometric measurements. *Journal of Vision*, 9(14):50.

Applegate, R. A., Marsack, J. D., Ramos, R., and Sarver, E. J. (2003). Interaction between aberrations to improve or reduce visual performance. *Journal of Cataract & Refractive Surgery*, 29(8):1487–1495.

Applegate, R. A., Marsack, J. D., and Thibos, L. N. (2006). Metrics of retinal image quality predict visual performance in eyes with 20/17 or better visual acuity. *Optometry and Vision Science*, 83(9):635–640.

Artal, P. (2017). *Handbook of Visual Optics, Volume Two: Instrumentation and Vision Correction.* Taylor & Francis.

Artal, P., Chen, L., Fernandez, E. J., Singer, B., Manzanera, S., and Williams, D. R. (2004). Neural compensation for the eye's optical aberrations. *Journal of Vision*, 4(4):281–7.

Artal, P., Marcos, S. C., Fonolla Navarro, R., Miranda, I., and Ferro, M. (1995). Through focus image quality of eyes implanted with monofocal and multifocal intraocular lenses. *Optical Engineering*, 34(3):772–779.

Atchison, D. and Smith, G. (2000). *Optics of the Human Eye*. Butterworth-Heinemann.

Atchison, D. A., Bradley, A., Thibos, L. N., and Smith, G. (1995). Useful variations of the badal optometer. *Optometry and Vision Science*, 72(4):279–284.

Atchison, D. A., Charman, W. N., and Woods, R. L. (1997). Subjective depth-of-focus of the eye. *Optometry and Vision Science*, 74(7):511–20.

Atchison, D. A., Fisher, S. W., Pedersen, C. A., and Ridall, P. G. (2005). Noticeable, troublesome and objectionable limits of blur. *Vision Research*, 45(15):1967–74.

Atchison, D. A., Guo, H., Charman, W. N., and Fisher, S. W. (2009a). Blur limits for defocus, astigmatism and trefoil. *Vision Research*, 49(19):2393–403.

Atchison, D. A., Guo, H., and Fisher, S. W. (2009b). Limits of spherical blur determined with an adaptive optics mirror. *Ophthalmic and Physiological Optics*, 29(3):300–311.

Atchison, D. A. and Mathur, A. (2011). Visual acuity with astigmatic blur. *Optometry and Vision Science*, 88(7):E798–805.

Atchison, D. A., Woods, R. L., and Bradley, A. (1998). Predicting the effects of optical defocus on human contrast sensitivity. *Journal of the Optical Society of America*, 15(9):2536–2544.

Augusteyn, R. C. (2007). Growth of the human eye lens. *Molecular Vision*, 13:252–257.

Bach, M. (1996). The freiburg visual acuity test–automatic measurement of visual acuity. *Optometry and Vision Science*, 73(1):49–53.

Bach, M. (2007). The freiburg visual acuity test-variability unchanged by post-hoc re-analysis. *Graefe's Archive for Clinical and Experimental Ophthalmology*, 245(7):965–971.

Bailey, I. L. and Lovie-Kitchin, J. E. (2013). Visual acuity testing. from the laboratory to the clinic. *Vision Research*, 90:2–9.

Bara, S., Arines, J., Ares, J., and Prado, P. (2006). Direct transformation of zernike eye aberration coefficients between scaled, rotated, and/or displaced pupils. *Journal of the Optical Society of America*, 23(9):2061–2066.

Barten, P. (1987). The sqri method - a new method for the evaluation of visible resolution on a display. In *Proceedings of the SID*, volume 28, pages 253–262.

Barten, P. G. (1999). *Contrast sensitivity of the human eye and its effects on image quality*, volume 72. SPIE press.

Barten, P. G. J. (1990). Evaluation of subjective image quality with the square-root integral method. *Journal of the Optical Society of America*.

Baumeister, M., Bühren, J., and Kohnen, T. (2009). Tilt and decentration of spherical and aspheric intraocular lenses: Effect on higher-order aberrations. *Journal of Cataract & Refractive Surgery*, 35(6):1006–1012.

Bellucci, R., Scialdone, A., Buratto, L., Morselli, S., Chierego, C., Criscuoli, A., Moretti, G., and Piers, P. (2005). Visual acuity and contrast sensitivity comparison between tecnis and acrysof sa60at intraocular lenses: a multicenter randomized study. *Journal of Cataract & Refractive Surgery*, 31(4):712–717.

Benard, Y., Lopez-Gil, N., and Legras, R. (2010). Subjective depth of field in presence of 4th-order and 6th-order zernike spherical aberration using adaptive optics technology. *Journal of Cataract & Refractive Surgery*, 36(12):2129–38.

Benard, Y., Lopez-Gil, N., and Legras, R. (2011). Optimizing the subjective depth-of-focus with combinations of fourth- and sixth-order spherical aberration. *Vision Research*, 51(23-24):2471–7.

Benjamin, W. J. (2006). *Borish's clinical refraction*, volume 2. Butterworth-Heinemann St. Louis.

Bennett, A. G. and Rabbetts, R. B. (1998). *Bennett and Rabbetts' clinical visual optics*. Elsevier Health Sciences.

Bodis-Wollner, I., Marx, M. S., Mitra, S., Bobak, P., Mylin, L., and Yahr, M. (1987). Visual dysfunction in parkinson's disease: loss in spatiotemporal contrast sensitivity. *Brain*, 110(6):1675–1698.

Bourne, R. R., Stevens, G. A., White, R. A., Smith, J. L., Flaxman, S. R., Price, H., Jonas, J. B., Keeffe, J., Leasher, J., Naidoo, K., et al. (2013). Causes of vision loss worldwide, 1990–2010: a systematic analysis. *The lancet global health*, 1(6):339–349.

Bradley, A., Thomas, T., Kalaher, M., and Hoerres, M. (1991). Effects of spherical and astigmatic defocus on acuity and contrast sensitivity: a comparison of three clinical charts. *Optometry & Vision Science*, 68(6):418–426.

Brindley, G. (1954). The summation areas of human colour-receptive mechanisms at increment threshold. *The Journal of Physiology*, 124(2):400–408.

Buehren, T. and Collins, M. J. (2006). Accommodation stimulusresponse function and retinal image quality. *Vision Research*, 46(10):1633–1645.

Campbell, C. E. (2003). Matrix method to find a new set of zernike coefficients from an original set when the aperture radius is changed. *Journal of the Optical Society of America*, 20(2):209–217.

Campbell, F. W. (1957). The depth of field of the human eye. *Optica Acta: International Journal of Optics*, 4(4):157–164.

Campbell, F. W. and Green, D. G. (1965). Optical and retinal factors affecting visual resolution. *The Journal of Physiology*, 181(3):576–593.

Campbell, F. W. and Robson, J. G. (1968). Application of fourier analysis to the visibility of gratings. *The Journal of Physiology*, 197(3):551–566.

Chan, C., Smith, G., and Jacobs, R. J. (1985). Simulating refractive errors: source and observer methods. *American Journal of Optometry and Physiological Optics*, 62(3):207–216.

Charman, W. and Jennings, J. (1976). Objective measurements of the longitudinal chromatic aberration of the human eye. *Vision Research*, 16(9):999–1005.

Charman, W. N. (1979). Effect of refractive error in visual tests with sinusoidal gratings. *The British Journal of Physiological Optics*, 33(2):10–20.

Charman, W. N. (2008). The eye in focus: accommodation and presbyopia. *Clinical and Experimental Optometry*, 91(3):207–225.

Charman, W. N., Adnan, and Atchison, D. A. (2012). Gradients of refractive index in the crystalline lens and transient changes in refraction among patients with diabetes. *Biomedical Optics Express*, 3(12):3033–3042.

Chen, A.-H. and O'Leary, A. P. D. J. (1998). Validity and repeatability of the modified push-up method for measuring the amplitude of accommodation. *Clinical and Experimental Optometry*, 81(2):63–71.

Cheng, X., Thibos, L. N., and Bradley, A. (2003). Estimating visual quality from wavefront aberration measurements. *Journal of Refractive Surgery*, 19(5):S579–S584.

CIE (1994). *Light as a True Visual Quantity: Principles of Measurement*, volume 41. Commission internationale de l'eclairage.

Cline, D., Hofstetter, H. W., and Griffin, J. R. (1997). *Dictionary of visual science*. Butterworth-Heinemann.

Collins, M. J., Brown, B., and Bowman, K. J. (1989). Contrast sensitivity with contact lens corrections for presbyopia. *Ophthalmic and Physiological Optics*, 9(2):133–138.

Cornelissen, P., Richardson, A., Mason, A., Fowler, S., and Stein, J. (1995). Contrast sensitivity and coherent motion detection measured at photopic luminance levels in dyslexics and controls. *Vision Research*, 35(10):1483–1494.

Curry, T. A., Sivak, J. G., Callender, M. G., and Irving, E. L. (1999). Afocal magnification does not influence chick eye development. *Optometry and Vision Science*, 76(5):316–319.

de Gracia, P., Dorronsoro, C., Gambra, E., Marin, G., Hernandez, M., and Marcos, S. (2010). Combining coma with astigmatism can improve retinal image over astigmatism alone. *Vision Research*, 50(19):2008–2014.

de Gracia, P., Marcos, S., Mathur, A., and Atchison, D. A. (2011). Contrast sensitivity benefit of adaptive optics correction of ocular aberrations. *Journal of vision*, 11(12):5.

Dehnert, A., Bach, M., and Heinrich, S. P. (2011). Subjective visual acuity with simulated defocus. *Ophthalmic and Physiological Optics*, 31(6):625–631.

Del Aguila-Carrasco, A. J., Marin-Franch, I., Bernal-Molina, P., Esteve-Taboada, J. J., Kruger, P. B., Montes-Mico, R., and Lopez-Gil, N. (2017). Accommodation responds to optical vergence and not defocus blur aloneaccommodation responds to optical vergence. *Investigative Ophthalmology & Visual Science*, 58(3):1758–1763.

Dorr, M., Lesmes, L. A., Elze, T., Wang, H., Lu, Z.-L., and Bex, P. J. (2017). Evaluation of the precision of contrast sensitivity function assessment on a tablet device. *Scientific Reports*, 7.

Dorr, M., Lesmes, L. A., Lu, Z.-L., and Bex, P. J. (2013). Rapid and reliable assessment of the contrast sensitivity function on an ipadipad contrast sensitivity function assessment. *Investigative Ophthalmology & Visual Science*, 54(12):7266–7273.

Dressler, M. and Rassow, B. (1981). Neural contrast sensitivity measurements with a laser interference system for clinical and screening application. *Investigative Ophthalmology & Visual Science*, 21(5):737–744.

Enroth-Cugell, C. and Robson, J. G. (1966). The contrast sensitivity of retinal ganglion cells of the cat. *The Journal of Physiology*, 187(3):517–552.

Esteve-Taboada, J. J., Del Aguila-Carrasco, A. J., Bernal-Molina, P., Lopez-Gil, N., Montes-Mico, R., Kruger, P., and Marin-Franch, I. (2017). Dynamic accommodation without feedback does not respond to isolated blur cues. *Vision Research*, pages 50–56.

Evans, K. K. and Treisman, A. (2005). Perception of objects in natural scenes: is it really attention free? *Journal of Experimental Psychology: Human Perception and Performance*, 31(6):1476–92.

Faul, F., Erdfelder, E., Lang, A. G., and Buchner, A. (2007). G*power 3: a flexible statistical power analysis program for the social, behavioral, and biomedical sciences. *Behavior Research Methods*, 39(2):175–91.

Fechner, T. G. (1860). *Elemente der Psychophysik*, volume 1. Breitkopf & Härtel.

Fernández, E., Iglesias, I., and Artal, P. (2001). Closed-loop adaptive optics in the human eye. *Optics letters*, 26(10):746–748.

Ferrer-Blasco, T., Gonzalez-Meijome, J. M., and Montes-Mico, R. (2008). Age-related changes in the human visual system and prevalence of refractive conditions in patients attending an eye clinic. *Journal of Cataract & Refractive Surgery*, 34(3):424–32.

Fincham, E. F. (1951). The accommodation reflex and its stimulus. *The British Journal of Ophthalmology*, 35(7):381–393.

Francisco Castejon-Mochon, J., Lopez-Gil, N., Benito, A., and Artal, P. (2002). Ocular wave-front aberration statistics in a normal young population. *Vision Research*, 42(13):1611–1617.

Gescheider, G. A. (1997). *Psychophysics: The fundamentals*, volume 3. Taylor & Francis.

Glasser, A., Croft, M. A., and Kaufman, P. L. (2001). Aging of the human crystalline lens and presbyopia. *International Ophthalmology Clinics*, 41(2):1–15.

Goertz, A. D., Stewart, W. C., Burns, W. R., Stewart, J. A., and Nelson, L. A. (2014). Review of the impact of presbyopia on quality of life in the developing and developed world. *Acta Ophthalmol*, 92(6):497–500.

Goodman, J. W. and Gustafson, S. C. (1996). *Introduction to fourier optics*, volume 35. International Society for Optics and Photonics.

Green, D. G., Powers, M. K., and Banks, M. S. (1980). Depth of focus, eye size and visual acuity. *Vision Research*, 20(10):827–35.

Gu, H., Kim, W., Hou, F., Lesmes, L. A., Pitt, M. A., Lu, Z.-L., and Myung, J. I. (2016). A hierarchical bayesian approach to adaptive vision testing: A case study with the contrast sensitivity function. *Journal of vision*, 16(6):15.

Guarnieri, F. (2014). *Corneal Biomechanics and Refractive Surgery*. Springer.

Guirao, A. and Williams, D. R. (2003). A method to predict refractive errors from wave aberration data. *Optometry and Vision Science*, 80(1):36–42.

Gullstrand, A. (1924). *Procedure of the rays in the eye. Imagery-laws of first order.* Optical Society of America, 3 edition.

Hartmann, J. (1900). Bermerkungen über den bau und die justierung von spektrographen. *Zeitschrift für Instrumentenkunde*, 20:47.

Hartridge, H. (1946). Visual acuity of the eye using lights of different colour. *The Journal of Physiology*, 105:2.

Hartwig, A. and Atchison, D. A. (2012). Analysis of higher-order aberrations in a large clinical population. *Investigative Ophthalmology & Visual Science*, 53(12):7862–70.

Hashemi, H., Khabazkhoob, M., Jafarzadehpur, E., Yekta, A., Emamian, M. H., Shariati, M., and Fotouhi, A. (2015). Higher order aberrations in a normal adult population. *Journal of Current Ophthalmology*, 27(3):115–124.

Hayashi, K., Hayashi, H., Nakao, F., and Hayashi, F. (2000). Influence of astigmatism on multifocal and monofocal intraocular lenses. *American Journal of Ophthalmology*, 130(4):477–82.

He, J. C., Burns, S. A., and Marcos, S. (2000). Monochromatic aberrations in the accommodated human eye. *Vision Research*, 40(1):41–48.

Helmholtz, v. H. (1867). *Handbuch der physiologischen Optik*, volume 9. Voss.

Holden, B. A. et al. (2007). Uncorrected refractive error: the major and most easily avoidable cause of vision loss. *Community Eye Health*, 20(63):37–9.

Holden, B. A., Fricke, T. R., Ho, S. M., Wong, R., Schlenther, G., Cronjé, S., Burnett, A., Papas, E., Naidoo, K. S., and Frick, K. D. (2008). Global vision impairment due to uncorrected presbyopia. *Archives of ophthalmology*, 126(12):1731–1739.

Howarth, P. A. and Bradley, A. (1986). The longitudinal chromatic aberration of the human eye, and its correction. *Vision research*, 26(2):361–366.

Huber, C. (1981a). *Myopic Astigmatism: A Substitute for Accommodation in Pseudophakia*. Junk.

Huber, C. (1981b). Planned myopic astigmatism as a substitute for accommodation in pseudophakia. *Journal - American Intra-Ocular Implant Society*, 7(3):244–9.

Huygens, C. (1690). *Tractatus de lumine*.

Iskander, D. R. (2006). Computational aspects of the visual strehl ratio. *Optometry and Vision Science*, 83(1):57–59.

ISO 20473:2007 (2007). Optics and Photonics Spectral Bands. Standard, International Organization for Standardization, Geneva, Switzerland.

ISO 8596:2017 (2017). Ophthalmic optics Visual acuity testing Standard and clinical optotypes and their presentation. Standard, International Organization for Standardization, Geneva, Switzerland.

Jansonius, N. M. and Kooijman, A. C. (1998). The effect of spherical and other aberrations upon the modulation transfer of the defocussed human eye. *Ophthalmic and Physiological Optics*, 18(6):504–513.

Johnson, C. A. and Casson, E. J. (1995). Effects of luminance, contrast, and blur on visual acuity. *Optometry and Vision Science*, 72(12):864–869.

Kadlecova, V., Peleska, M., and Vasko, A. (1958). Dependence on age of the diameter of the pupil in the dark. *Nature*, 182(4648):1520–1521. 10.1038/1821520a0.

Kandel, E. R., Schwartz, J. H., Jessell, T. M., Siegelbaum, S. A., and Hudspeth, A. J. (2000). *Principles of neural science*, volume 4. McGraw-hill.

Kasper, T., Bühren, J., and Kohnen, T. (2006). Visual performance of aspherical and spherical intraocular lenses: Intraindividual comparison of visual acuity, contrast sensitivity, and higher-order aberrations. *Journal of Cataract & Refractive Surgery*, 32(12):2022–2029.

Kelly, D. (1973). Lateral inhibition in human colour mechanisms. *The Journal of Physiology*, 228(1):55–72.

Kim, J. Y., Alarcon, A., and Yoon, G. (2014). Improving binocular through focus visual performance by inducing different interocular orientation of astigmatism. *Investigative Ophthalmology & Visual Science*, 55(5):5972.

Kingdom, F. A. A. and Prins, N. (2010). *Psychophysics: a practical introduction*. Academic Press London.

Kleiner, M., Brainard, D., Pelli, D., Ingling, A., Murray, R., and Broussard, C. (2007). Whats new in psychtoolbox-3. *Perception*, 36(14):1–16.

Kleiner, R. C., Enger, C., Alexander, M. F., and Fine, S. L. (1988). Contrast sensitivity in age-related macular degeneration. *Archives of Ophthalmology*, 106(1):55–57.

Kruger, P. B., Nowbotsing, S., Aggarwala, K. R., and Mathews, S. (1995). Small amounts of chromatic aberration influence dynamic accommodation. *Optometry and Vision Science*, 72(9):656–666.

Kruger, P. B. and Pola, J. (1986). Stimuli for accommodation: blur, chromatic aberration and size. *Vision Research*, 26(6):957–971.

Le Grand, Y. (1964). *Optique physiologique: La dioptrique de l'oeil et sa correction. Tome premier*. Masson.

Lee, J. H., Stark, L. R., Cohen, S., and Kruger, P. B. (1999). Accommodation to static chromatic simulations of blurred retinal images. *Ophthalmic and Physiological Optics*, 19(3):223–235.

Legge, G. E., Mullen, K. T., Woo, G. C., and Campbell, F. W. (1987). Tolerance to visual defocus. *Journal of the Optical Society of America. A, Optics, Image Science, and Vision*, 4(5):851–863.

Legras, R. and Benard, Y. (2013). Measurement and prediction of subjective gradations of images in presence of monochromatic aberrations. *Vision Research*, 86:52–58.

Legras, R., Benard, Y., and Lopez-Gil, N. (2012). Effect of coma and spherical aberration on depth-of-focus measured using adaptive optics and computationally blurred images. *Journal of Cataract & Refractive Surgery*, 38(3):458–469.

Legras, R., Chateau, N., and Charman, W. N. (2004). Assessment of just-noticeable differences for refractive errors and spherical aberration using visual simulation. *Optometry and Vision Science*, 81(9):718–728.

Lesmes, L. A., Lu, Z.-L., Baek, J., and Albright, T. D. (2010). Bayesian adaptive estimation of the contrast sensitivity function: The quick csf method. *Journal of Vision*, 10(3):17.

Leube, A., Ohlendorf, A., and Wahl, S. (2016a). The influence of induced astigmatism on the depth of focus. *Optometry and Vision Science*, 93(10):1228–1234.

Leube, A., Ohlendorf, A., and Wahl, S. (2016b). Sign-dependent response of visual acuity and contrast sensitivity to spherical defocus. In *Visual and Physiological Optics*. Antwerp.

Leube, A., Ohlendorf, A., and Wahl, S. (2016c). Wavefront-based 3-dimensional refraction from objective visual strehl metrics. In *Young Researcher Vision Camp*. Leibertingen.

Leube, A., Tabernero, J., Ohlendorf, A., and Wahl, S. (2015). Relationship between the subjectively and objectively determined depth of focus of the human eye using defocus curves. *Investigative Ophthalmology & Visual Science*, 56(7):6016.

Liang, J., Grimm, B., Goelz, S., and Bille, J. F. (1994). Objective measurement of wave aberrations of the human eye with the use of a hartmann–shack wave-front sensor. *Journal of the Optical Society of America*, 11(7):1949–1957.

Lieberman, H. R. and Pentland, A. P. (1982). Microcomputer-based estimation of psychophysical thresholds: the best pest. *Behavior Research Methods*, 14(1):21–25.

Lu, Q., Congdon, N., He, X., Murthy, G. V., Yang, A., and He, W. (2011). Quality of life and near vision impairment due to functional presbyopia among rural chinese adults. *Investigative ophthalmology & visual science*, 52(7):4118–4123.

Lundstrom, L., Gustafsson, J., and Unsbo, P. (2007). Vision evaluation of eccentric refractive correction. *Optometry and Vision Science*, 84(11):1046–1052.

Lundstrom, L. and Unsbo, P. (2007). Transformation of zernike coefficients: scaled, translated, and rotated wavefronts with circular and elliptical pupils. *Journal of the Optical Society of America. A, Optics, Image Science, and Vision*, 24(3):569–577.

Marcos, S., Burns, S. A., Moreno-Barriusop, E., and Navarro, R. (1999a). A new approach to the study of ocular chromatic aberrations. *Vision Research*, 39(26):4309–4323.

Marcos, S., Moreno, E., and Navarro, R. (1999b). The depth-of-field of the human eye from objective and subjective measurements. *Vision Research*, 39(12):2039–49.

Marcos, S., Werner, J. S., Burns, S. A., Merigan, W. H., Artal, P., Atchison, D. A., Hampson, K. M., Legras, R., Lundstrom, L., Yoon, G., Carroll, J., Choi, S. S., Doble, N., Dubis, A. M., Dubra, A., Elsner, A., Jonnal, R., Miller, D. T., Paques, M., Smithson, H. E., Young, L. K., Zhang, Y., Campbell, M., Hunter, J., Metha, A., Palczewska, G., Schallek, J., and Sincich, L. C. (2017). Vision science and adaptive optics, the state of the field. *Vision Research*, 132:3–33.

Marsack, J. D., Thibos, L. N., and Applegate, R. A. (2004). Metrics of optical quality derived from wave aberrations predict visual performance. *Journal of Vision*, 4(4):8.

Mathews, S. and Kruger, P. B. (1994). Spatiotemporal transfer function of human accommodation. *Vision Research*, 34(15):1965–1980.

McLellan, J. S., Marcos, S., and Burns, S. A. (2001). Age-related changes in monochromatic wave aberrations of the human eye. *Investigative Ophthalmology & Visual Science*, 42(6):1390–1395.

Michael, R., Guevara, O., de la Paz, M., Alvarez de Toledo, J., and Barraquer, R. I. (2011). Neural contrast sensitivity calculated from measured total contrast sensitivity and modulation transfer function. *Acta Ophthalmologica*, 89(3):278–283.

Michelson, A. (1927). *Studies in optics*. University of Chicago.

Mishkin, M., Ungerleider, L. G., and Macko, K. A. (1983). Object vision and spatial vision: two cortical pathways. *Trends in Neurosciences*, 6:414–417.

Mon-Williams, M., Tresilian, J. R., Strang, N. C., Kochhar, P., and Wann, J. P. (1998). Improving vision: neural compensation for optical defocus. *Proceedings of the Royal Society B: Biological Sciences*, 265(1390):71–77.

Montés-Micó, R. and Alió, J. L. (2003). Distance and near contrast sensitivity function after multifocal intraocular lens implantation. *Journal of Cataract & Refractive Surgery*, 29(4):703–711.

Mordi, J. A. and Ciuffreda, K. J. (1998). Static aspects of accommodation: age and presbyopia. *Vision Research*, 38(11):1643–1653.

Nagpal, K. M., Desai, C., Trivedi, R. H., and Vasavada, A. R. (2000). Is pseudophakic astigmatism a desirable goal? *Indian Journal of Ophthalmology*, 48(3):213–6.

Naidoo, K. S., Leasher, J., Bourne, R. R., Flaxman, S. R., Jonas, J. B., Keeffe, J., Limburg, H., Pesudovs, K., Price, H., White, R. A., Wong, T. Y., Taylor, H. R., Resnikoff, S., and Vision Loss Expert Group of the Global Burden of Disease, S. (2016). Global vision impairment and blindness due to uncorrected refractive error, 1990-2010. *Optom Vis Sci*, 93(3):227–34.

Navarro, R. and Losada, M. A. (1997). Aberrations and relative efficiency of light pencils in the living human eye. *Optometry and Vision Science*, 74(7):540–547.

Nio, Y. K., Jansonius, N. M., Fidler, V., Geraghty, E., Norrby, S., and Kooijman, A. C. (2000). Age-related changes of defocus-specific contrast sensitivity in healthy subjects. *Ophthalmic Physiological Optics*, 20(4):323–34.

Ogle, K. N. and Schwartz, J. T. (1959). Depth of focus of the human eye. *Journal of the Optical Society of America*, 49(3):273–80.

Ohlendorf, A. and Schaeffel, F. (2009). Contrast adaptation induced by defocus - a possible error signal for emmetropization? *Vision Research*, 49(2):249–256.

Ohlendorf, A., Tabernero, J., and Schaeffel, F. (2011). Visual acuity with simulated and real astigmatic defocus. *Optometry and Vision Science*, 88(5):562–9.

Pedrotti, F., Pedrotti, L., Bausch, W., and Schmidt, H. (2007). *Optik für Ingenieure: Grundlagen*. Springer Berlin Heidelberg.

Peli, E. (1997). In search of a contrast metric: Matching the perceived contrast of gabor patches at different phases and bandwidths. *Vision Research*, 37(23):3217–3224.

Pieh, S., Lackner, B., Hanselmayer, G., Zohrer, R., Sticker, M., Weghaupt, H., Fercher, A., and Skorpik, C. (2001). Halo size under distance and near conditions in refractive multifocal intraocular lenses. *British Journal of Ophthalmology*, 85(7):816–21.

Platt, B. C. and Shack, R. (2001). History and principles of shack-hartmann wavefront sensing. *Journal of Refractive Surgery*, 17(5):S573–S577.

Pokorny, J., Graham, C. H., and Lanson, R. (1968). Effect of wavelength on foveal grating acuity. *Journal of the Optical Society of America*, 58(10):1410–1414.

Prez-Merino, P., Birkenfeld, J., Dorronsoro, C., Ortiz, S., Durn, S., Jimnez-Alfaro, I., and Marcos, S. (2014). Aberrometry in patients implanted with accommodative intraocular lenses. *American Journal of Ophthalmology*, 157(5):1077–1089.

Raasch, T. W. (1995). Spherocylindrical refractive errors and visual acuity. *Optometry and Vision Science*, 72(4):272–5.

Radhakrishnan, H., Pardhan, S., Calver, R. I., and O'Leary, D. J. (2004a). Effect of positive and negative defocus on contrast sensitivity in myopes and non-myopes. *Vision Research*, 44(16):1869–1878.

Radhakrishnan, H., Pardhan, S., Calver, R. I., and O'Leary, D. J. (2004b). Unequal reduction in visual acuity with positive and negative defocusing lenses in myopes. *Optometry and Vision Science*, 81(1):14–7.

Ravikumar, S., Thibos, L. N., and Bradley, A. (2008). Calculation of retinal image quality for polychromatic light. *Journal of the Optical Society of America*, 25(10):2395–2407.

Resnikoff, S., Pascolini, D., Mariotti, S. P., and Pokharel, G. P. (2008). Global magnitude of visual impairment caused by uncorrected refractive errors in 2004. *Bulletin of the World Health Organization*, 86(1):63–70.

Roaf, H. (1930). Visual acuity in light of different colours. *Proceedings of the Royal Society of London. Series B, Containing Papers of a Biological Character*, 106(744):276–292.

Rocha, K. M., Soriano, E. S., Chamon, W., Chalita, M. R., and Nosé, W. (2007). Spherical aberration and depth of focus in eyes implanted with aspheric and spherical intraocular lenses: A prospective randomized study. *Ophthalmology*, 114(11):2050–2054.

Rocha, K. M., Vabre, L., Chateau, N., and Krueger, R. R. (2009). Expanding depth of focus by modifying higher-order aberrations induced by an adaptive optics visual simulator. *Journal of Cataract & Refractive Surgery*, 35(11):1885–1892. 0886-3350.

Rynders, M., Navarro, R., and Losada, M. (1998). Objective measurement of the off-axis longitudinal chromatic aberration in the human eye. *Vision Research*, 38(4):513–522.

Santamaría, J., Artal, P., and Bescós, J. (1987). Determination of the point-spread function of human eyes using a hybrid optical–digital method. *Journal of the Optical Society of America*, 4(6):1109–1114.

Savage, H., Rothstein, M., Davuluri, G., El Ghormli, L., and Zaetta, D. M. (2003). Myopic astigmatism and presbyopia trial. *American Journal of Ophthalmology*, 135(5):628–632.

Sawusch, M. R. and Guyton, D. L. (1991). Optimal astigmatism to enhance depth of focus after cataract surgery. *Ophthalmology*, 98(7):1025–9.

Schade, O. H. (1956). Optical and photoelectric analog of the eye. *Journal of the Optical Society of America*, 46(9):721–739.

Schaeffel, F., Wilhelm, H., and Zrenner, E. (1993). Inter-individual variability in the dynamics of natural accommodation in humans: relation to age and refractive errors. *The Journal of Physiology*, 461:301–320.

Schilling, T., Ohlendorf, A., Leube, A., and Wahl, S. (2017). Tuebingencstesta useful method to assess the contrast sensitivity function. *Biomedical Optics Express*, 8(3):1477–1487.

Schmid, K. L., Strang, N. C., and Wildsoet, C. F. (1999). Imposed retinal image size changes-do they provide a cue to the sign of lens-induced defocus in chick? *Optometry and Vision Science*, 76(5):320–325.

Schmidinger, G., Geitzenauer, W., Hahsle, B., Klemen, U. M., Skorpik, C., and Pieh, S. (2006). Depth of focus in eyes with diffractive bifocal and refractive multifocal intraocular lenses. *Journal of Cataract & Refractive Surgery*, 32(10):1650–6.

Schultze, M. (1866). Zur anatomie und physiologie der retina. *Archiv für mikroskopische Anatomie*, 2(1):175–286.

Schwarz, C., Canovas, C., Manzanera, S., Prieto, P. M., Weeber, H., Piers, P., and Artal, P. (2012). Depth of focus with induced coma at different orientations. *Investigative Ophthalmology & Visual Science*, 53(14):6329.

Schwiegerling, J. (2002). Scaling zernike expansion coefficients to different pupil sizes. *Journal of the Optical Society of America*, 19(10):1937–1945.

Sehlapelo, R. and Oduntan, A. (2007). Effect of optical defocus on colour perception. *The South African Optometrist*, 66(2):77–81.

Seidemann, A. and Schaeffel, F. (2002). Effects of longitudinal chromatic aberration on accommodation and emmetropization. *Vision Research*, 42(21):2409–2417.

Shack, R. V. and Platt, B. (1971). Production and use of a lenticular hartmann screen. In *Journal of the Optical Society of America*, volume 61, page 656.

Sheedy, J. E., Campbell, C., King-Smith, E., and Hayes, J. R. (2005). Progressive powered lenses: the minkwitz theorem. *Optometry and Vision Science*, 82(10):916–22.

Stiles, W. (1946). A modified helmholtz line-element in brightness-colour space. *Proceedings of the Physical Society*, 58(1):41.

Stiles, W. S. and Crawford, B. H. (1933). The luminous efficiency of rays entering the eye pupil at different points. *Proceedings of the Royal Society of London. Series B, Containing Papers of a Biological Character*, 112(778):428–450.

Stuart, G. W., McAnally, K. I., and Castles, A. (2001). Can contrast sensitivity functions in dyslexia be explained by inattention rather than a magnocellular deficit? *Vision Research*, 41(24):3205–3211.

Tarrant, J., Roorda, A., and Wildsoet, C. F. (2010). Determining the accommodative response from wavefront aberrations. *Journal of Vision*, 10(5):4.

Thibos, L., Bradley, A., Still, D., Zhang, X., and Howarth, P. (1990). Theory and measurement of ocular chromatic aberration. *Vision Research*, 30(1):33–49.

Thibos, L. N., Applegate, R. A., Schwiegerling, J. T., and Webb, R. (2002a). Standards for reporting the optical aberrations of eyes. *Journal of Refractive Surgery*, 18(5):S652–5660.

Thibos, L. N., Bradley, A., and Zhang, X. (1991). Effect of ocular chromatic aberration on monocular visual performance. *Optometry and Vision Science*, 68(8):599–607.

Thibos, L. N., Hong, X., Bradley, A., and Applegate, R. A. (2004). Accuracy and precision of objective refraction from wavefront aberrations. *Journal of Vision*, 4(4):329–51.

Thibos, L. N., Hong, X., Bradley, A., and Cheng, X. (2002b). Statistical variation of aberration structure and image quality in a normal population of healthy eyes. *Journal of the Optical Society of America*, 19(12):2329–2348.

Thibos, L. N., Wheeler, W., and Horner, D. (1997). Power vectors: an application of fourier analysis to the description and statistical analysis of refractive error. *Optometry and Vision Science*, 74(6):367–75.

Thibos, L. N., Ye, M., Zhang, X., and Bradley, A. (1992). The chromatic eye: a new reduced-eye model of ocular chromatic aberration in humans. *Applied Optics*, 31(19):3594–3600.

Treisman, A. (1986). Features and objects in visual processing. *Scientific American*, 255(5):114–125.

Trindade, F., Oliveira, A., and Frasson, M. (1997). Benefit of against-the-rule astigmatism to uncorrected near acuity. *Journal of Cataract & Refractive Surgery*, 23(1):82–5.

Tucker, J. and Charman, W. (1975). The depth-of-focus of the human eye for snellen letters. *American Journal of Optometry and Physiological Optics*, 52(1):3–21.

Ungerleider, L. G. and Haxby, J. V. (1994). what and where in the human brain. *Current Opinion in Neurobiology*, 4(2):157–165.

Vasudevan, B., Ciuffreda, K. J., and Wang, B. (2006). An objective technique to measure the depth-of-focus in free space. *Graefe's Archive for Clinical and Experimental Ophthalmology*, 244(8):930–7.

Villegas, E. A., Alcon, E., and Artal, P. (2008). Optical quality of the eye in subjects with normal and excellent visual acuity. *Investigative Ophthalmology & Visual Science*, 49(10):4688–4696.

Vinas, M., Sawides, L., de Gracia, P., and Marcos, S. (2012). Perceptual adaptation to the correction of natural astigmatism. *PLoS One*, 7(9):e46361.

Wahl, S., Fornoff, L., Ochakovski, G. A., and Ohlendorf, A. (2017). Disability glare in soft multifocal contact lenses. *Contact Lens and Anterior Eye*.

Wald, G. (1968). The molecular basis of visual excitation. *Nature*, 219:800–807.

Wang, B. and Ciuffreda, K. J. (2006). Depth-of-focus of the human eye: theory and clinical implications. *Survey of Ophthalmology*, 51(1):75–85.

Watson, A. B. and Ahumada, A. J. (2008). Predicting visual acuity from wavefront aberrations. *Journal of Vision*, 8(4):17.

Weale, R. A. (1961). The duplicity theory of vision: Edridge-green lecture delivered at the royal college of surgeons of england on 28th march 1959. *Annals of the Royal College of Surgeons of England*, 28(1):16.

WHO (2006). Sight test and glasses could dramatically improve the lives of 150 million people with poor vision. *Indian J Med Sci*, 60(11):485–6.

Wildsoet, C. F., Howland, H. C., Falconer, S., and Dick, K. (1993). Chromatic aberration and accommodation: their role in emmetropization in the chick. *Vision Research*, 33(12):1593–1603.

Williams, D., Yoon, G. Y., Porter, J., Guirao, A., Hofer, H., and Cox, I. (2000). Visual benefit of correcting higher order aberrations of the eye. *Journal of Refractive Surgery*, 16(5):554–559.

Winn, B., Whitaker, D., Elliott, D. B., and Phillips, N. J. (1994). Factors affecting light-adapted pupil size in normal human subjects. *Investigative Ophthalmology & Visual Science*, 35(3):1132–1137.

Wyszecki, G. and Stiles, W. (2000). *Color Science: Concepts and Methods, Quantitative Data and Formulae*. Wiley.

Xu, R., Bradley, A., and Thibos, L. N. (2013). Impact of primary spherical aberration, spatial frequency and stiles crawford apodization on wavefront determined refractive error: a computational study. *Ophthalmic and Physiological Optics*, 33(4):444–455.

Yao, P., Lin, H., Huang, J., Chu, R., and Jiang, B.-c. (2010). Objective depth-of-focus is different from subjective depth-of-focus and correlated with accommodative microfluctuations. *Vision Research*, 50(13):1266–1273. 0042-6989.

Yi, F., Iskander, D. R., and Collins, M. (2011). Depth of focus and visual acuity with primary and secondary spherical aberration. *Vision Research*, 51(14):1648–58.

Yi, F., Iskander, D. R., and Collins, M. J. (2010). Estimation of the depth of focus from wavefront measurements. *Journal of Vision*, 10(4):3 1–9.

Yoon, G.-Y. (2010). The use of adaptive optics to study optical and neural impact on visual performance. In *Frontiers in Optics 2010/Laser Science XXVI*, OSA Technical Digest (CD). Optical Society of America.

Zele, A. J. and Cao, D. (2015). Vision under mesopic and scotopic illumination. *Frontiers in Psychology*, 5:1594.

9 Publications, conference contributions and talks related to this work

9.1 Peer reviewed publications

Ohlendorf Arne, **Leube Alexander** & Wahl Siegfried (2016). Steps towards smarter solutions in optometry and ophthalmology: inter-device agreement of subjective methods to assess the refractive errors of the eye. Healthcare 4(41): 1-11. doi:10.3390/healthcare4030041

Schilling Tim, Ohlendorf Arne, **Leube Alexander** & Wahl Siegfried (2017). TuebingenCSTest A useful method to assess the contrast sensitivity function. Biomedical Optics Express, 8(3): 1477-1487. doi: 10.1364/BOE.8.001477

Leube Alexander, Rifai Katharina & Wahl Siegfried (2017). Sampling rate influences saccade detection in mobile eye tracking of a reading task. Journal of Eye Movement Research, 10(3): 1-11. doi: 10.16910/jemr.10.3.3

Leube Alexander, Kovats Imre, Wahl Siegfried & Sickenberger Wolfgang (2017). Axis-free correction of astigmatism using bifocal soft contact lenses. Contact Lens and Anterior Eye. 40(6): 394-400. doi: 10.1016/j.clae.2017.09.002

Leube Alexander, Kraft Caroline, Ohlendorf Arne & Wahl Siegfried (2018). Self-assessment of refractive errors using a simple optical approach. Clinical and Experimental Optometry. doi: 10.1111/cxo.12650

9.2 Peer reviewed conference contributions

Leube Alexander, Ohlendorf Arne, Tabernero Juan & Wahl Siegfried (2015). Relationship between the subjectively and objectively determined depth of focus of the human eye using defocus curves. Investigative Ophthalmology & Visual Science. 56, 6016. ARVO, Denver (USA).

Ohlendorf Arne, **Leube Alexander**, Wahl Siegfried (2015). The effect of an cycloplegic agent on the objectively and subjectively determined refraction. Investigative Ophthalmology & Visual Science. 56, 525. ARVO, Denver (USA).

Lange Heike, **Leube Alexander**, Vogel Mandy, Ohlendorf Arne, Wahl Siegfried, Wiedemann Peter, Wieland Kiess & Rauscher Franziska (2016). Prevalence of refractive errors in a large German cohort of children. Investigative Ophthalmology & Visual Science. 57, 3974. ARVO, Seattle (USA)

Leube Alexander, Schilling Tim, Ohlendorf Arne & Wahl Siegfried (2016). Evaluating the goodness of various equations to model the contrast sensitivity function. Investigative Ophthalmology & Visual Science, 213. ARVO, Seattle (USA).

Leube Alexander, Ohlendorf Arne & Wahl Siegfried (2016). Wavefront-based 3-dimensional Refraction from Objective Visual Strehl Metrics. YRVC, Leibertingen (Germany).

Leube Alexander, Kern David, Ohlendorf Arne & Wahl Siegfried (2017). Radial averaging of the optical modulation transfer function and its impact on image quality. Investigative Ophthalmology & Visual Science. 58, 1123. ARVO, Baltimore (USA).

Ohlendorf Arne, **Leube Alexander**, Leibig Christian & Wahl Siegfried (2017). A machine learning approach to determine refractive errors of the eye. Investigative Ophthalmology & Visual Science. 58, 1136. ARVO, Baltimore (USA).

Leube Alexander, Rifai Katharina & Wahl Siegfried (2017). Mobile eye tracking: Reliability in assessing saccadic eye movements in reading. 19th European Conference on Eye Movements, Wuppertal (Germany).

Ohlendorf Arne, Kostial Stephanie, **Leube Alexander** & Wahl Siegfried (2017). Sensitivity to defocus in myopes under monochromatic lighting conditions. 16th International Myopia Conference, Birmingham (UK).

9.3 Peer reviewed talks

Leube Alexander (2016). Sign-dependent response of visual acuity and contrast sensitivity to spherical defocus. Visual and Physiological Optics, Antwerpen (Belgium).

9.4 Non peer reviewed talks

Leube Alexander (2015). Defokuskurven zur Ermittlung der Schärfentiefe des menschlichen Auges. Sommerkolloquium Ernst-Abbe-Hochschule Jena (Germany).

Leube Alexander (2015). Defokuskurven in der Ophthalmologie und Optometrie Ein Update. Arbeitskreis Ophthalmologische Optik, Jena (Germany).

Leube Alexander, Ohlendorf Arne (2016). Assessment of image quality in optical systems. Progress in Ophthalmic Research. Institute for Ophthalmic Research, Eberhard-Karls University Tübingen (Germany).

Leube Alexander (2016). Sphero-zylindrische Selbstrefraktion - Eigenständige Bestimmung der sphero-zylindrischen Refraktion mit Hilfe von Alvarez Linsen. Arbeitskreis Ophthalmologische Optik, Tübingen (Germany).

Leube Alexander (2017). Vorzeichenabhängige Reduktion der Sehschärfe unter monochromatischen Lichtbedingungen. Arbeitskreis Ophthalmologische Optik, Erlangen (Germany).

10 Statement of own contribution

10.1 Publication 1 - The influence of induced astigmatism on the depth of focus

Leube, A., Ohlendorf, A., & Wahl, S. (2016). The Influence of Induced Astigmatism on the Depth of Focus. Optometry and Vision Science, 93(10), 1228-1234. doi: 10.1097/OPX.0000000000000961

Contribution of the first author:

I developed the initial idea for the experiments and selected and developed the methods. I recruited the subjects, performed the measurements, and analyzed the data. I wrote the first version of the manuscript and continued to improve it based on my ideas and input from the other authors.

Contribution of the other authors:

The second author of the paper, Dr. Arne Ohlendorf, supported the work with his experience in planning and performing experiments and helped to improve the manuscript. The third author, Prof. Siegfried Wahl, was available for discussions, suggestions and helped to improve the various versions of the manuscript.

10.2 Publication 2 - Individual neural transfer function affects the prediction of subjective depth of focus

Leube, A., Schilling, T., Ohlendorf, A., Kern, D., Ochakovski, A. G., Fischer, M. D., & Wahl, S. (2018). Individual neural transfer function affects the prediction of subjective depth of focus. Scientific Reports, 8(1), 1919. doi: 10.1038/s41598-018-20344-x

Contribution of the first author:

I developed the initial idea for the experiments and selected and developed the methods. I recruited the subjects, performed the measurements, and analyzed the data. I wrote the first version of the manuscript and continued to improve it based on my ideas and input from the other authors.

Contribution of the other authors:

The second and the third author of the paper, Dr. Arne Ohlendorf and Tim Schilling, supported the work with the development of a precise test for the contrast sensitivity of the human eye and helped to improve the manuscript. The fourth author of the paper, David Kern, helped with the data acquisition and analyzing the data. The fifth and the sixth author of the paper, Alex Ochakovski and Prof. M. Dominik Fischer, are ophthalmologists at the university eye clinic of Tübingen and performed the ophthalmological pre-examination of the participants and the application of the cycloplegic eye drops. The last author, Prof. Siegfried Wahl, was available for discussions, suggestions and helped to improve the various versions of the manuscript.

10.3 Publication 3 - Symmetric visual response to positive and negative induced spherical defocus under monochromatic light conditions

Leube, A., Kostial, S., Alex Ochakovski, G., Ohlendorf, A., & Wahl, S. (2018). Symmetric visual response to positive and negative induced spherical defocus under monochromatic light conditions. Vision Research, 143, 52-57. doi: 10.1016/j.visres.2017.12.003

Contribution of the first author:

I developed the initial idea for the experiments and selected and developed the methods. I recruited the subjects, performed the measurements, and analyzed the data. I wrote the first version of the manuscript and continued to improve it based on my ideas and input from the other authors.

Contribution of the other authors:

The second author of the paper, Stephanie Kostial, helped with the data aquisition and analyzing the data. The third author, Dr. Arne Ohlendorf, supported the work with helpful discussions and improvements of the manuscript. The fourth author of the paper, Alex Ochakovski, is an ophthalmologists at the university eye clinic of Tübingen and performed the ophthalmological pre-examination of the participants and the application of the cycloplegic eye drops. The last author, Prof. Siegfried Wahl, was available for discussions, suggestions and helped to improve the various versions of the manuscript.

11 Acknowledgements

Firstly, I would like to express my sincere gratitude to my advisors Prof. Dr. Frank Schaeffel and Prof. Dr. Siegfried Wahl for their continuous support of my doctoral studies and related research, for their patience, motivation, and immense knowledge. Their guidance helped me throughout the entire time of research and writing of this thesis.

Besides my advisors, I wish to express my deepest gratitude to Dr. Arne Ohlendorf as my post-doctoral mentor, for his support, insightful comments and encouragement during the entire period of research. He supported me in all stages of the doctoral studies with inspiration and positive criticism on my laboratory work and the joined scientific publications and he always makes me feel welcome. I could not have imagined a better mentor for my doctoral studies.

I would also like to thank all the members of the ZEISS Vision Science Lab Tübingen, especially Cote, for the profound and valuable discussions and their immense contribution to my personal and professional success in the last four years. I have had the pleasure to work with and supervise the thesis of three master students, Caroline Kraft, David Kern and Stephanie Kostial, whom I would like to acknowledge their enthusiasm and contributions regarding the help in data acquisition. I further want to thank all the volunteers for participating in the experiments.

For the support and the help of the optical calculations I would like to thank Prof. Larry N. Thibos from the Indiana University, Bloomington and Dr. Juan Tabernero from the Anglia Ruskin University, Cambridge. Their openness and willingness to answer my questions and provide their help in technical respects contributed significantly to this work.

Finally, I would like to thank my family for all their love and encouragement. I am deeply grateful for my parents who raised me with an open mind and supported me in all of my pursuits. Thank you.